Fermilab

TM-1155 Revised

1183.000

MAGNET DESIGN STUDY FROM THE CONCEPTUAL DESIGN REPORT FOR THE DIRECT NEUTRAL LEPTON FACILITY*

Edited by T. Murphy

May 1985

This supersedes TM-1155.

I. Introduction

This appendix is an updated version of TM-1155, by C. Baltay, et al. (October, 1982), which was the original design report for this facility. Outdated sections have been deleted, and a new section describing the redesign to 900 GeV incident protons has been added. (TM-1155 was a design for 1000 GeV incident protons.) The appendices to TM-1155, which contain the actual equations used in the Monte Carlo programs, have also been omitted.

The main technical challenge in the design of the Direct Neutral Lepton Facility is the magnetized muon shield. Muon backgrounds have been calculated by three independent computer programs at Columbia, Fermilab, and MIT. The calculated background fluxes are satisfactory in all of the detectors that might use the facility (i.e., the Tohoku and 15 Foot Bubble Chambers, as well as counter detectors located in Lab E and Lab C). The spoiler design includes a conventional iron magnet system with an air gap in the central regions of high muon flux. Detailed engineering design has been carried out by various departments at Fermilab on this design including detailed calculations of the magnetic field shapes and estimates of costs.

To check the reliability of the programs used in the design of the muon shield, we have calculated the background muon fluxes in the E-613 muon shield in the Meson Lab for a variety of conditions. We found that the agreement between the measured fluxes and the fluxes calculated by the three independent programs is quite satisfactory. These results were reported in June 1982 to the Fermilab Directorate. The programs reproduce satisfactorily the detailed distributions of the muon flux measured by E-613 at the end plane of the iron shield and at the front face of the detector. The programs also permitted a calculation of a factor of ~5 reduction in the muon flux measured with the modified version of the shield used in the spring 1982 run of E-613. In fact, this reduction factor was predicted by one of the programs before the shield was modified and the fluxes were measured. We therefore have confidence that the programs give realistic results to within a factor of two. In view of the safety factor of ~10 in the design for the 15 Foot and Tohoku chambers, this seems quite satisfactory.

In Section II of this report we describe in detail the three Monte Carlo programs used in these calculations. In Section III we give the details of the flux calculations for the E-613 shield and the comparisons with the observed fluxes with various configurations of the shield. In Section IV we describe the designs that have been developed for the neutrino area shield. The 1984 redesign to 900 GeV incident protons is described in Section V. In Section VI we discuss the problem of proton beam transport loss and the associated muon fluxes.

II. Description of the Monte Carlo Programs

The difficulties and uncertainties in predicting the background muon rate leaking through an active muon shield for a beam dump experiment are by now well known. In order to increase confidence in the design of a Tevatron beam dump facility each experimental group with Program Advisory Committee approval as well as the design group within Fermilab have developed a program for this calculation. The three programs have been written independently, though discussions between the groups have frequently contributed to the understanding of the effects involved.

The following sections will discuss the various effects included in the three programs. Detailed equations are included in an appendix to TM-1155.

Each of the three programs takes a different approach to the calculation of muon production by protons incident on a heavy target. The Columbia and Fermilab programs treat muon production in two stages: pion production and either pion decay or direct muon production expressed as a fraction of pion production. The MIT program directly expresses muon production from all sources.

The pion production formulas used in the Columbia and Fermilab programs derive from the radial scaling fits to pion production data from many p $p \rightarrow \pi^{\pm}$ X experiments at various energies up to 400 GeV. These fits extend to a P_t of 6 GeV/c for π^+ and somewhat lower for π^-. In the Fermilab program a correction is made to give agreement with ISR data at still larger P_t, out to 10 GeV/c. Since radial scaling gives excellent fits to data over a wide range of incident proton energies, it is expected that the interpolation to 1 TeV will be satisfactory.

The calculation of pion decay to muons in a material of given interaction length is straight forward. The ratio of direct muon production to pion production has been measured in several experiments at Fermilab. The general result is that the μ/π ratio is independent of P_t at small x and falls with x as a power of $(1-x)$. The Columbia formula uses $(1-x)^3$ and the Fermilab program $(1-x)^2$. Either form gives a reasonable fit to the measurements.

The product of pion production and either the pion decay probability or the μ/π ratio gives the rate of muon production by the primary proton beam. In a thick target such as the beam dump re-interaction of produced pions and protons are an important contribution to the total. The Columbia program carries out a shower Monte Carlo for each production interaction. In this calculation secondary pions are allowed to interact and produce either more pions or direct muons. The Fermilab program uses an enhancement factor as a function of p_π/p_{beam} that is derived from a separate shower Monte Carlo calculation.

This calculation allows secondary pions to interact as in the Columbia program, but in addition one forward secondary nucleon is

generated and allowed to interact. This calculation follows the shower to a depth of 3 in the pions and 6 in the nucleons.

Finally, both the Columbia and Fermilab calculations must correct from production in pp collisions to that in pA collisions where A may be Be, Fe, Cu, or W. For this purpose an approximate A dependence of the pion invariant cross sections as given by L. Voyvodic is applied. In addition, the μ/π ratio should increase as $A^{0.2}$ since pion production rises more slowly than direct muon production.

The MIT program does not attempt to determine muon production from a stepwise calculation but relies instead upon a fit to total muon production from a W target as generated by W. Busza. That formula includes both direct and decay muons from all generations of the shower in a thick target. Figure II-1 shows the total muon production rate as a function of momentum from 400 GeV protons incident on iron. In Figure II-2, the rate has been scaled to tungsten.

All three of the programs under discussion make use of standard techniques to follow the central trajectory of a produced muon from the target through the absorbers and magnets of a particular shield design. The Columbia and Fermilab programs generate initial muon momenta and directions randomly and weight according to the production spectrum discussed above. The MIT program proceeds more systematically, stepping in P_t and p until all of phase space is covered. Comparisons of trajectories for particular initial conditions have indicated good agreement among the programs in the calculation of magnetic bending.

A muon that would not strike the detectors if it were not deflected may nonetheless produce a hit if it undergoes one of a number of processes along its path. The first such process considered in the programs is multiple Coulomb scattering. In the Columbia and MIT programs Coulomb scattering is normally treated by calculating the undeflected ray and determining where it would strike the plane of a detector. The total Coulomb scattering angle is calculated and the probability of a hit by this central ray is determined by an integration of the 2-dimensional scattering probability distribution over the area of the detector. In contrast, the Fermilab program changes the direction of a muon according to the Coulomb scattering distribution appropriate to the thickness of material traversed in one step of the path integration.

An important observation is that for large thickness, such as the entire dump, a Gaussian distribution is an excellent approximation to the true Coulomb distribution. For small steps the Moliere tails must be taken into account. The Fermilab program does this in a way that crudely accounts for the nuclear form factor but includes the effects of large angle plural scattering. The Gaussian distribution and the Moliere tails are plotted in Figure II-3.

A second effect that can cause an otherwise "safe" muon trajectory to strike a detector is inelastic muon scattering in the material of the

dump. The Fermilab program determines the effect of inelastic muon scattering by producing a scatter at a random point along the trajectory and then following the deviated path. Scatters are generated uniformly in and within chosen limits. This is to ensure that all regions of the scattering distribution are sampled adequately. The scattering probability is converted to a weight and multiplies the production weight of the muon to give the final weight added to the total to give the number of hits on a detector.

In the MIT program, inelastic scattering is taken account of by an integration over q^2 and ν carried out at many points along the path of a muon. The range in ν is determined taking into account the stopping power of the portion of the dump remaining between the scattering point and the detector. The integral accumulates the scattering probability for that portion of the kinematic space that leads to a hit on the detector. Figure II-4 compares calculations of the three programs with data from the EMC on the scattering of 280 GeV/c muons from 2.3m of iron.

A third process that can contribute to the background is electromagnetic trident production. This effect is particularly dangerous since it can lead to an effective change of sign of the muon and thus to a cancellation of the magnetic deflection achieved before the interaction. The spectrum is relatively hard, dropping as 1/p, so it is difficult to defeat this process by range. All three programs calculate the effects of trident formation by treating it as a special kind of inelastic scattering, but allowing for the possible sign change.

The Columbia and MIT programs both treat energy loss of the muons as they travel through the dump as a continuous process. The Columbia program allows for the energy dependence of dE/dx in iron but treats loss in dirt as a constant. The MIT program uses an equation that fits the calculated loss rate in iron as a function of energy and scales that formula to give the correct minimum loss rate for dirt. In the Fermilab program a table is constructed that includes the exact restricted energy loss calculation for each relevant process: ionization, electron pair production and bremstrahlung. This table contains dE/dx for each material at intervals of 1 GeV/c momentum up to 1 TeV/c. Only losses due to collisions in which less than 10% of the energy is lost are included in this table. A separate calculation randomly generates an occasional large stochastic energy loss from the range 10% to 100% of the incident energy. The values of dE/dx for the three programs are compared in Figure II-5.

In the Columbia and MIT programs, the magnetic fields in active elements of the dump are always entered in the form of detailed field maps. These maps have been derived from various sources, sometimes by hand calculation and sometimes by detailed calculation with programs such as POISSON. The Fermilab Monte Carlo has the capability to accept detailed field maps, but has usually been applied in a mode in which it is given the field in a series of regions on the midplane of a magnet and then calculates the vertical and horizontal return fields by applying

flux conservation. This calculation gives the uniform field that would return the central flux. If the iron of the return yoke is saturated a uniform field is a good approximation. For unsaturated return yokes a linear variation is added to give agreement with detailed calculations.

The actual equations used to describe the above processes may be found in TM-1155, p. 14-20, and this report, p. 27-32.

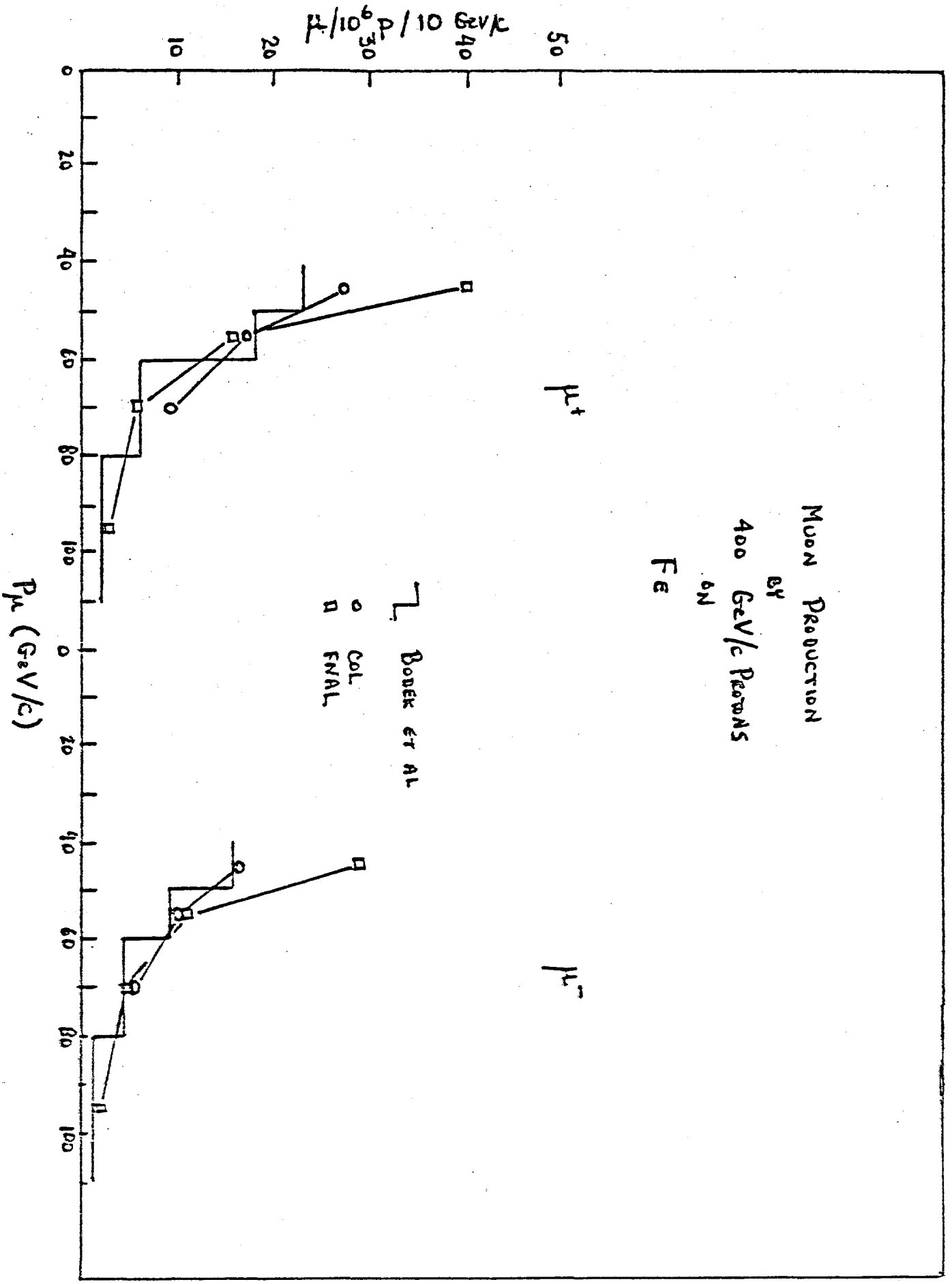
MUON PRODUCTION
BY
400 GeV/c PROTONS
ON
Fe
BODEK ET AL
COL
FNAL
μ+
μ-
μ/10⁶P/10 GeV/c
P_μ (GeV/c)

Fig. II-1

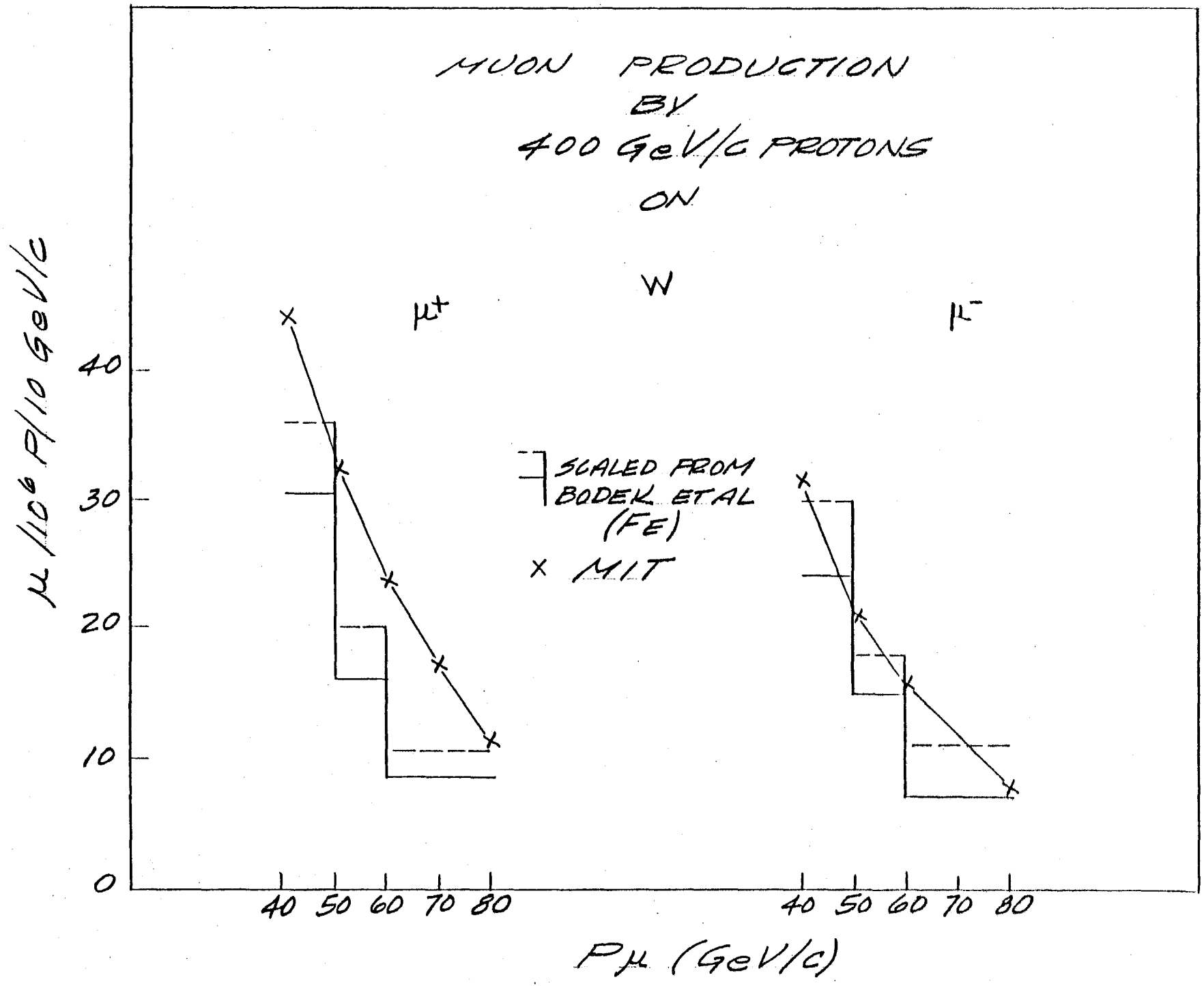
MUON PRODUCTION
BY
400 GeV/c PROTONS
ON
W
μ+
μ−
SCALED FROM
BODEK ET AL
(Fe)
× MIT
μ / 10^6 P/10 GeV/c
0
10
20
30
40
40 50 60 70 80
40 50 60 70 80
Pμ (GeV/c)

Fig. II-2

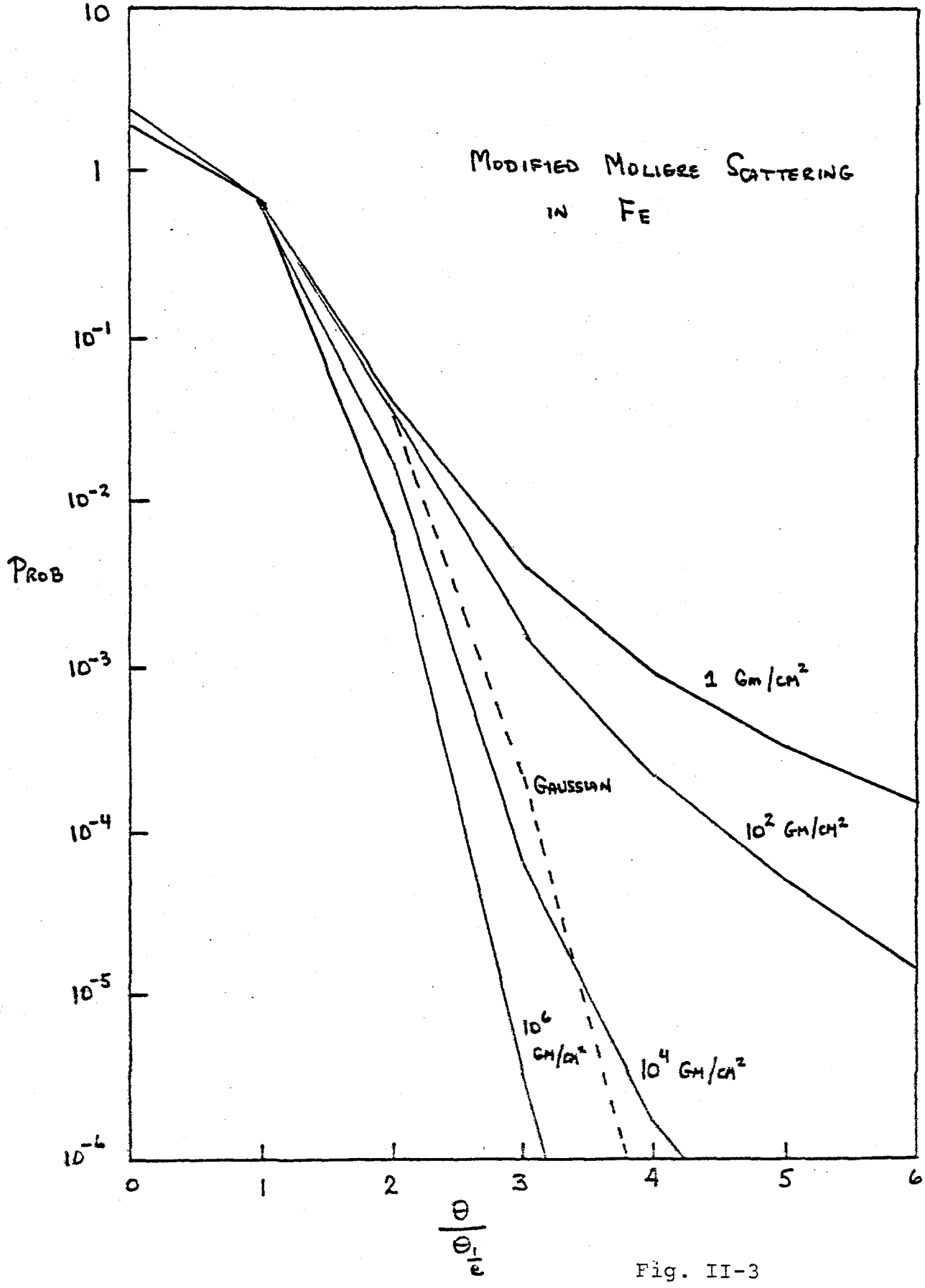
MODIFIED MOLIGEE SCATTERING
IN FE
PROB
10
1
10^-1
10^-2
10^-3
10^-4
10^-5
10^-6
0
1
2
3
4
5
6
θ / θ_1/e
1 GM/CM^2
10^2 GM/CM^2
GAUSSIAN
10^4 GM/CM^2
10^6 GM/CM^2

Fig. II-3

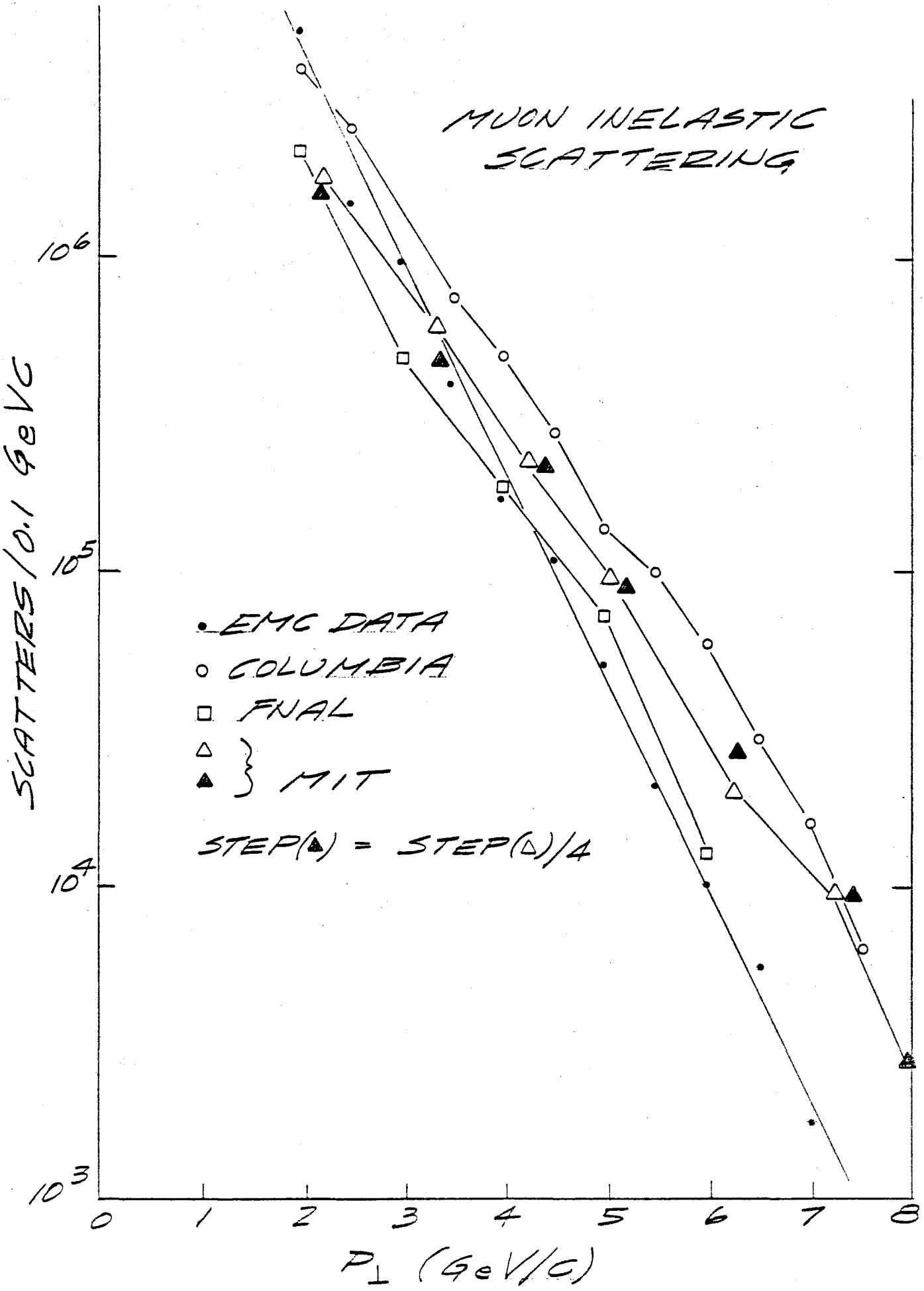
MUON INELASTIC SCATTERING
SCATTERS/0.1 GeV/c
10^6
10^5
10^4
10^3
• EMC DATA
○ COLUMBIA
□ FNAL
△ ▲ } MIT
STEP(▲) = STEP(△)/4
0
1
2
3
4
5
6
7
8
$P_\perp$ (GeV/c)

Fig. II-4

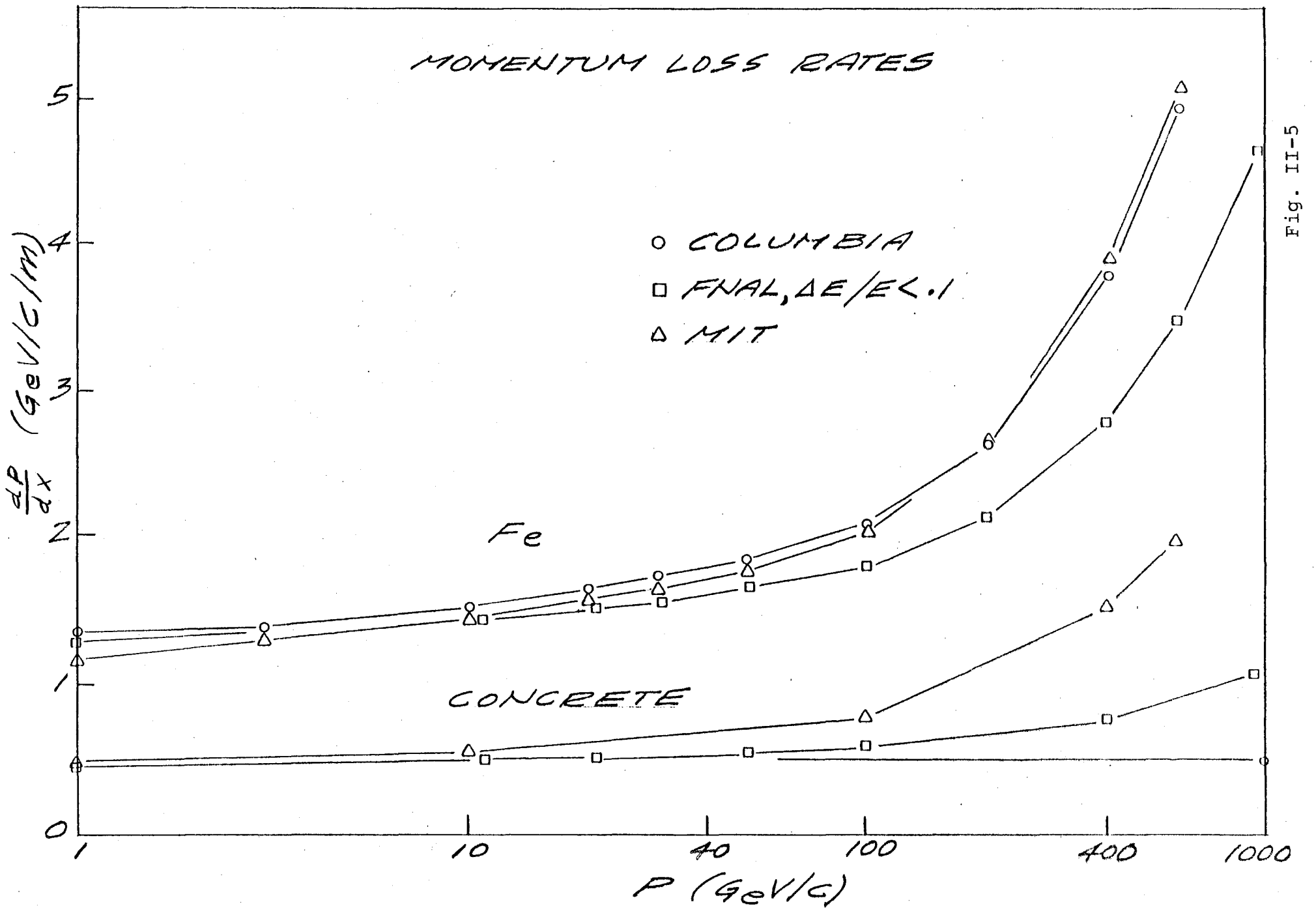
MOMENTUM LOSS RATES
COLUMBIA
FNAL, ΔE/E<.1
MIT
Fe
CONCRETE
dp/dx (GeV/c/m)
P (GeV/c)
0
1
2
3
4
5
1
10
40
100
400
1000

Fig. II-5

III. The E-613 Shield

The magnetized muon shield built for the beam dump experiment E-613 in the Meson Lab has some similarities to the shield we are designing for the Direct Neutral Lepton Facility in the neutrino area.

We felt that it would be a significant test of our programs to calculate the background muon fluxes in the E-613 shield and compare these to the actually measured muon fluxes. Such calculations have therefore been carried out using all three of the programs used in the neutrino area design for a variety of configurations of the E-613 shield. The agreement between the calculations and the measured fluxes is satisfactory for all three programs. In this section we describe these comparisons in some detail.

We have considered two different versions of this shield - the "Old Shield" used in the Spring 1981 run, and the "New Shield" used in the Spring 1982 run. In both versions the shield consisted of a magnetized iron front end followed by a passive iron shield. (See Figure III-1 for a sketch of these two versions). The magnetized part was the same for both versions and consisted of three magnets M1, M2, and the Hyperon magnet (10.4 meters total length) followed by two off-axis "spoiler" magnets. The passive part was approximately 13 meters long in the 1981 shield and about 18 meters long in the 1982 shield. Between the passive shield and the detector there was another 3 m long but narrower piece of passive iron (called the AVIS magnet) and 1.4 meters of concrete. Some parameters of these shields are summarized below:

	1981 Shield	1982 Shield
Length of magnetized iron[a]	10.4 m	10.4 m
Total B x L	223 Kgm	223 Kgm
ΔP_t	6.7 GeV/c	6.7 GeV/c
Total length of iron[b]	24 m	29 m
Minimum energy loss in shield	35 GeV	42 GeV
Multiple scatt. (ΔP_t)rms proj.	0.56 GeV/c	0.62 GeV/c

a) Excluding spoiler magnets.

b) Excluding spoiler magnets and AVIS iron

The muon flux measurements carried out with this shield are given in the May 4, 1982, note by S. Childress and B. Roe and a December 8, 1981, note by G.K. Fanourakis. The available data fall into four categories:

1. The muon anticounters (MUANTI) at the front face of the detector. They cover a total of 5 feet x 5 feet, consisting of five horizontal strips labeled A, B, C, D, E (See Figure III-1) which are 5 feet wide by 1 foot high each. These give the total muon flux hitting the detector.

2. A probe counter (P counter) which is about 7" x 10" in size at the end of the passive iron shield (~31 meters from target in 1981, ~36 meters from target in 1982) counting in coincidence with the MUANTI counters (called P• MUANTI). The P counter was moved up and down at the end of the shield, but was always centered horizontally on the beam axis. The P• MUANTI coincidence gives the vertical distribution at the end of the passive iron for muons that hit the detector. (See Figures III-2 to 5)

3. The singles counting rate with the P counters both at the end of the passive iron and in the plane of the front face of the detectors. In regions of very high counting rate these counts are probably related to the total muon flux. However in regions of low muon flux they may have substantial backgrounds, or may even be dominated by, hadronic or electromagnetic junk (they are singles counts in a 7" x 10" counter).

4. Muons seen in the E-613 detector in the time gate of a neutrino event trigger (called "stale muons"). These muons must have at least 1.1 GeV to be detected, and about 5 GeV to traverse the whole detector. Thus the muon flux between 1.1 and 5 GeV and the flux above 5 GeV in the detector are available.

Due to an error in stacking at the time when the 1981 shield was modified to the new 1982 configuration, too much iron (by six blocks) was placed on top of the passive iron shield. In this position the extra six blocks intercepted the very high flux of deflected muons, multiple scattered some of them into the detector, and thus increased the flux of muons in the detector. These blocks were then removed when the error was discovered, and the muon flux decreased by the expected factor of five or so. The fluxes were measured with all six blocks on, four of these blocks off, and finally with all six blocks off. In addition, the muon fluxes were measured by the E-613 group with the incident proton beam pitched upward by 4 milliradians ("PITCH ON" data), which was their usual running condition, and also with the incident protons at 0 milliradian (i.e. "PITCH OFF" data). Thus there exists a large amount of measured muon flux data under a large variety of conditions, i.e. the original 1981 configuration, the final 1982 configuration (with all six blocks off), and the two intermediate configurations (with all six blocks on, and with four blocks off, two on), each of these with the proton beam at 0 mrad and 4 mrad. We have calculated the expected muon fluxes for each of these configurations with each of the three programs (i.e. Columbia, Fermilab, and MIT) independently. The large variety of different conditions provided a fairly thorough check of the calculations.

The results of the calculations for the total muon fluxes (sum of μ^+ and μ^-) are compared with the E-613 measurements in Table III-1. The first column of the Table gives the measured fluxes, and columns 2, 3, and 4 give the fluxes calculated by the three programs. We see that the calculations are within a factor of two of each other and the measurements for all of the various conditions for which measurements are available. We consider this very satisfactory agreement.

The calculations of the vertical distribution of the muon flux at the end of the passive iron (for muons that also hit the detector) are compared with the P. MUANTI coincidence counts in Figures III-2 to III-5. Finally, the calculations for the vertical and horizontal distribution flux in the plane of the front face of the detector are compared with the corresponding P singles measurements in Fig. III-6 and III-7. The agreement between the calculations and the measurements is within a factor of three or so even in these detailed distributions, which we consider quite satisfactory.

However, a few comments about the precision of the agreement that can be expected might be useful.

a) The precision of the measured fluxes can be estimated by looking at the internal consistency of the measurements.

For example, consider the "PITCH OFF" data with the incident protons at 0 mrad to the horizontal. Since the 613 detector is vertically centered 30 cm above the horizontal axis, with the incident protons at 0 mrad the high energy end of the muons (300 to 400 GeV) clip the upper edge of the detectors. From the simple geometry of the situation we see that these muons pass the end plane of the passive iron shield (at 36 meters from the target) in a narrow region around 6 feet above the floor (see Fig. III-8). Such a peak is indeed observed and can be seen in Figures III-3,4,5. However both the magnitude and the position of this peak at 6 feet should be independent of the number of steel blocks above 9 feet on top of the shield. But the measured peak in Figures III-3 to 5 (Figures 9, 10, and 11 of May 4, 1982, note by Childress and Roe) vary by a factor of two in magnitude and 6" in position. We thus conclude that the precision (normalization, position, etc.) of the P• MUANTI measurements are no better than a factor of two in magnitude and 6" in position.

Another example worth looking at is the horizontal distribution of the muons above the detector (Fig. III-7, or Fig. 13 of the May 4, 1982 report by Childress and Roe) which shows a sharp peak about 20" off center. However, all of the relevant components of the beam and shield are claimed to be centered horizontally, so therefore our programs calculate a peak of magnitude comparable to the observed peak but centered horizontally. This indicates that either the placement of some of the shield or beam components or the position accuracy of the E-613 flux measurement are off by as much as 20".

b) In a detailed comparison of the inner workings of the three muon flux programs, we tried to separate the effects of the initial muon production rates in the dump from the calculation of the transmission of the shield. We define the transmission ratio at a particular set of initial values of the total momentum P and the transverse momentum P_t as the fraction of muons (produced in the dump at that P and P_t) that end up in the detector. This ratio is clearly independent of the number of muons produced at that P and P_t. Figs. III -9 and III-10 show the comparisons of the three programs at a few values of P and P_t. The agreement is well within a factor of two.

The three programs use different parameterizations of the pion production rates and of the μ/π ratios in the dump, as discussed in Section II of this appendix. The agreement between these parameterizations is not better than a factor of two. We therefore believe that the differences between the fluxes calculated by the three programs are mainly due to the muon production formulas and not because of differences in calculating what muons do in the shield. A detailed comparison of the predictions of the three programs and measured muon rates from 300 and 400 GeV proton-nucleon interactions can be found in TM-1155, p. 45-60. We reproduce here the most relevant part of that discussion. ← and this report, p. 33-36.

a. The most relevant data for the total muon production is the data of Bodek, Ritchie et al. In this experiment, the total $\mu^{\pm}$ production rate was measured with 350 GeV protons in an iron beam dump. Jack Ritchie was very kind to supply us with this data before corrections were subtracted for π,K decays, etc. These numbers then can be directly compared to the total muon rates from our formulae, which is the quantity that is relevant to us. His numbers were for 6.038×10^8 protons interacting in the dump. He thought that the data were reliable for the region $P_\mu \geq 50$ GeV and $P_t \geq 0.6$ GeV/c. The comparison for the x dependence is shown in Figures III-11 and 12 and the P_t dependence in Figures III-13 and 14. We see that the agreement is good, with the Columbia formulae overestimating by a factor of typically 1.5, and the MIT formula by ~2. But, note the data is for iron and the MIT prediction is for tungsten. Since the formulae predict more than the data, our calculations using these formulae will be conservative since we will calculate more background than we should actually have.

b. The comparison with the Bodek, Ritchie et al. data is very reassuring. It covers a fairly large range in x, out to x = 0.63. However, it is limited to $P_t \leq 2.2$ GeV/c. To check the high P_t fluxes, we compared with the CERN ISR data on π^o production in the CCOR experiment out to P_t ~14 GeV/c. The comparison of these data with the Taylor-Walker formula for π production used in the Columbia and the Fermilab program is shown in Figures III-15 and 16. The agreement is quite good at low P_t (as it should be) but at P_t ~10 GeV/c, which is the highest P_t that may be relevant in the muon shield calculations, the formula overestimates the measured

cross sections by a factor of five or so (at $\sqrt{s}$ = 53, which is similar to the Tevatron). Again, the calculations using this formula are then conservative since they overestimate the background. The formula used in the Fermilab program agree well with the data.

c. The highest P_t muon production data that we could find was that of Cronin et al. This was for inclusive μ^+ production by 300 GeV protons. The data available is for the prompt μ^+ production in a thin nuclear target, corrected for μ's from π and K decay. The comparison with the prompt μ cross section from the formula used in the Columbia program is shown in Figure III-17. The agreement is good at low P_t but the formula overestimates the measured cross section by almost an order of magnitude at P_t ~6 GeV/c. The MIT formula for the total μ^+ cross section is also shown (the prompt and the decay contributions cannot be separated in this formula) and is larger than the measured data. Thus the calculations based on these formulae can be expected to be conservative at high P_t. The formula used in the Fermilab program agrees very well in shape but the normalization is slightly low (but within a factor of two or so of the data).

In view of the above comments about the precision of the muon flux measurements, the positioning of the elements of the shield, and the uncertainties of the muon production formulas, we believe that the agreement between our calculations and the actually observed muon fluxes are quite satisfactory, both in the total fluxes and the detailed flux distributions.

Another point worth noting is that the factor of five decrease in the muon background flux in the E-613 detector due to the additional 5 meters of passive iron (the main change from the 1981 shield to the final 1982 shield configuration) was predicted by one of our programs before the shield was restacked and the reduced flux was measured. It gives us more confidence in our programs that they are not only able to explain fluxes after the observed rates are known but they can predict what will happen in some new configuration before the flux measurements are made. In addition, the set of muon measurements with full density tungsten target and the final shielding configuration was made after our muon flux predictions were made available for that configuration. The agreement is again satisfactory.

Table III-1

E-613 Shield Muon Flux Comparisons

	Observed Flux	Columbia Program	Fermilab Program	MIT Program
1. Old Shield (1981)				
Total MUANTI	47,500	56,000	40,000	58,500
$P_\mu \geq 1.1$ GeV/c	25,000	34,000		
Counter A	15,053	19,500	10,300	18,000
B	11,048	1,200	5,200	12,500
C	9,171	10,600	6,500	9,500
D	7,035	11,500	10,300	9,000
E	7,336	13,800	7,700	9,500
2. New Shield (1982)				
6 Blocks ON	58,000		48,000	53,000
4 Blocks OFF, 2 ON	29,000			20,000
Final (All 6 Blocks OFF)	10,400	6,200	5,400	8,000

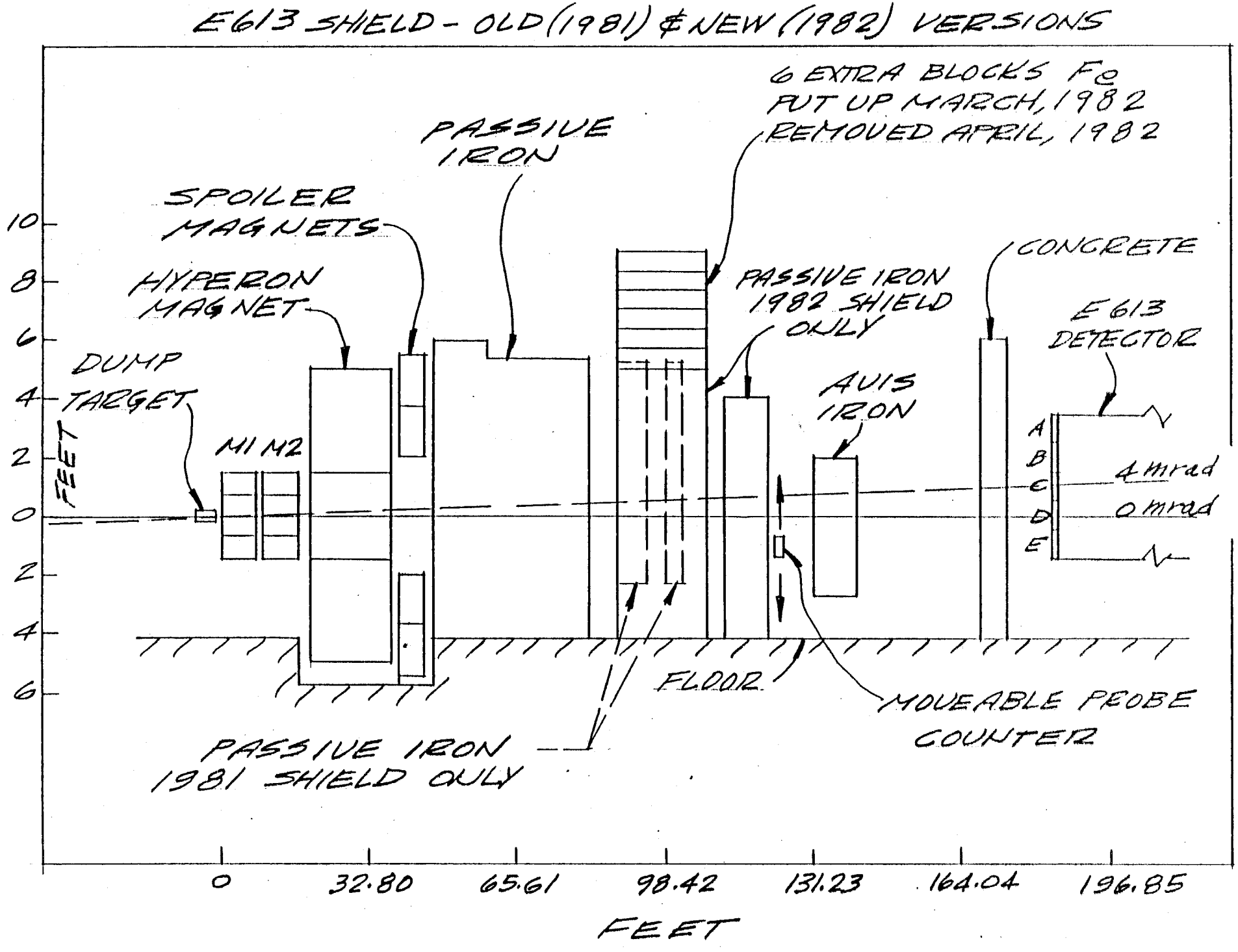
E613 SHIELD - OLD (1981) & NEW (1982) VERSIONS
6 EXTRA BLOCKS Fe
PUT UP MARCH, 1982
REMOVED APRIL, 1982
PASSIVE IRON
SPOILER MAGNETS
HYPERON MAGNET
DUMP TARGET
M1 M2
PASSIVE IRON 1982 SHIELD ONLY
AUIS IRON
CONCRETE
E613 DETECTOR
A
B
C
D
E
4 mrad
0 mrad
FEET
10
8
6
4
2
0
2
4
6
FLOOR
MOVEABLE PROBE COUNTER
PASSIVE IRON 1981 SHIELD ONLY
0
32.80
65.61
98.42
131.23
164.04
196.85
FEET

Fig. III-1

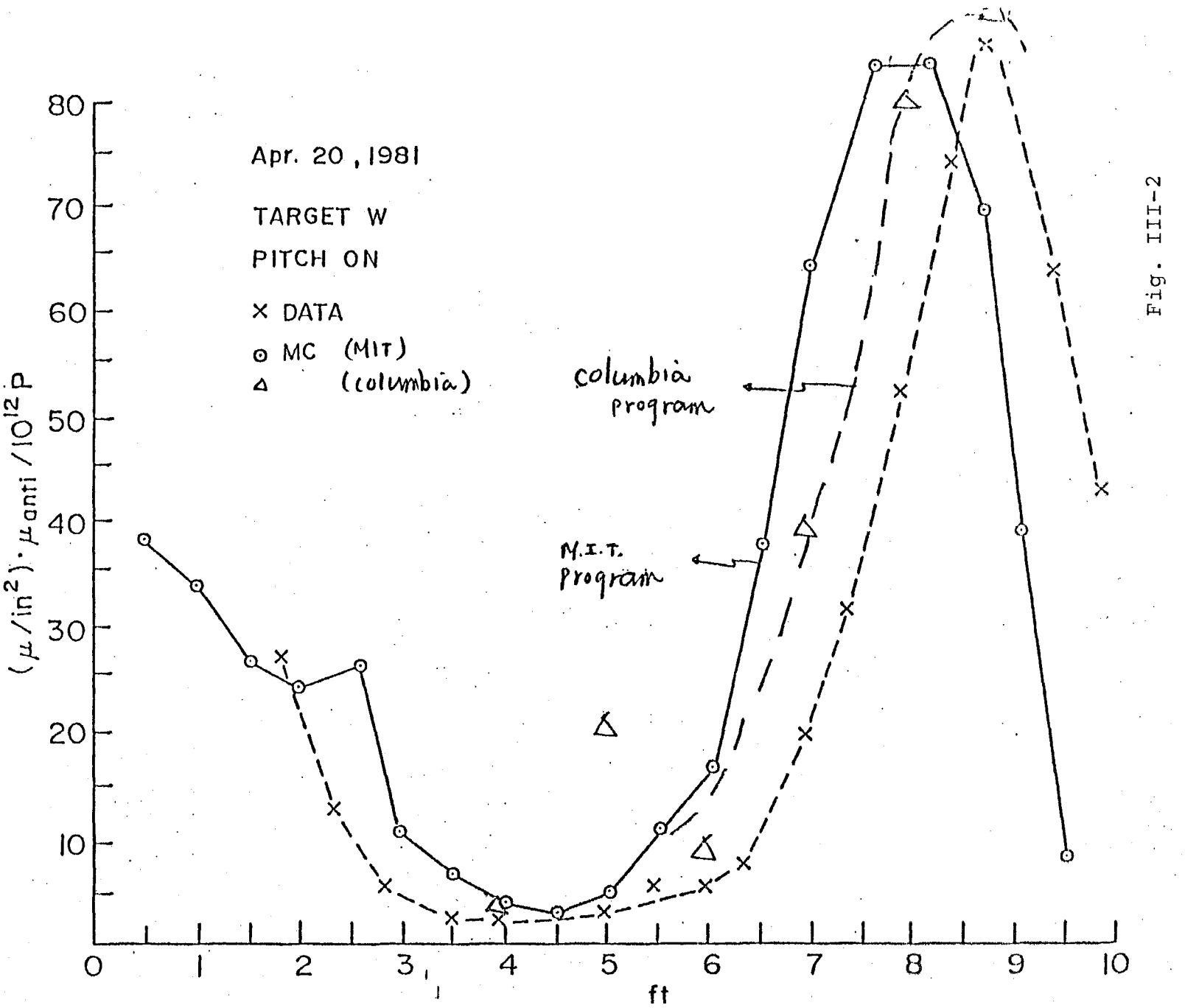
Apr. 20, 1981
TARGET W
PITCH ON
× DATA
⊙ MC (MIT)
△ (columbia)
columbia program
M.I.T. Program
(μ/in²)·μanti/10¹² p
ft
0
1
2
3
4
5
6
7
8
9
10
10
20
30
40
50
60
70
80

Fig. III-2

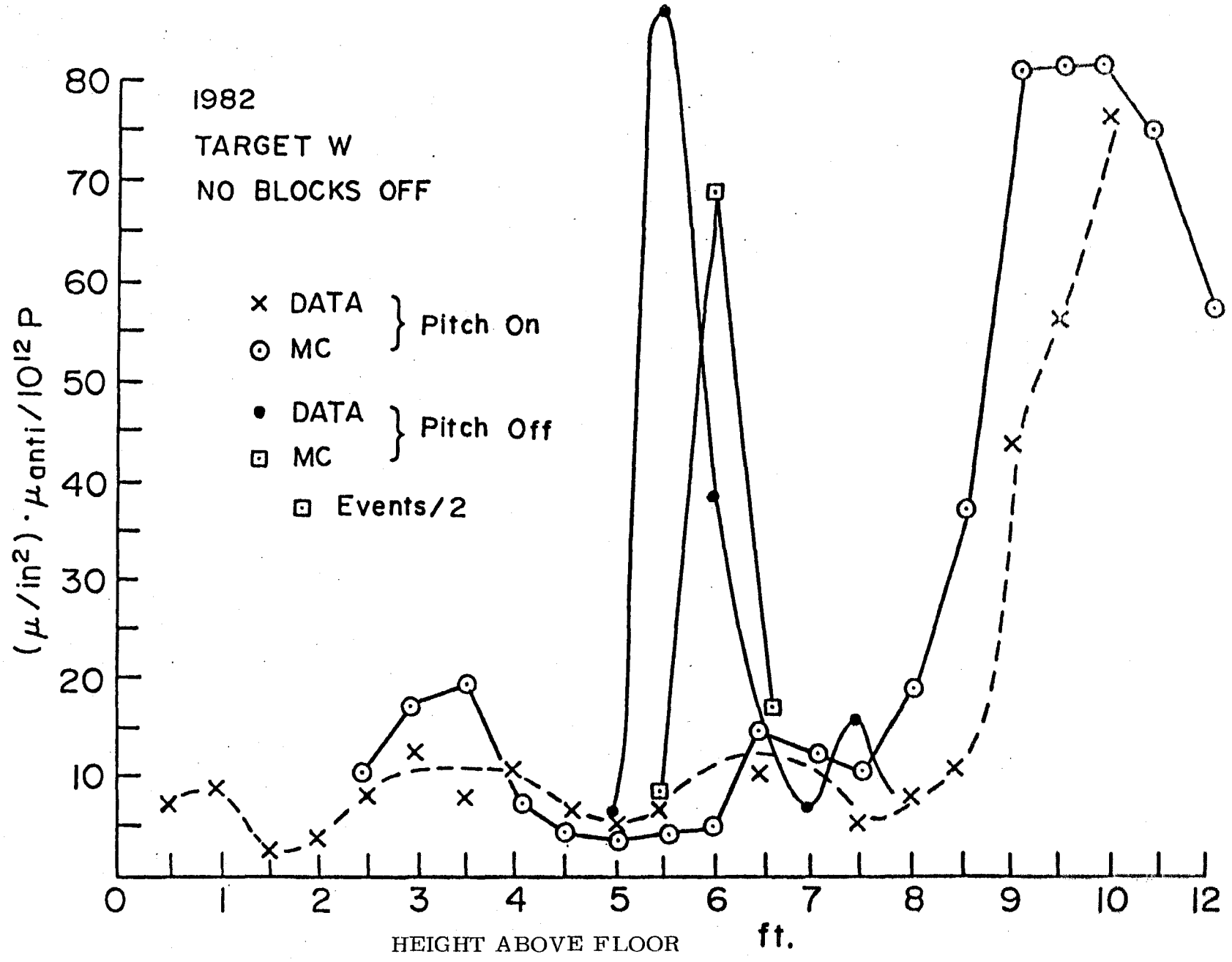
1982
TARGET W
NO BLOCKS OFF
× DATA
⊙ MC
Pitch On
• DATA
⊡ MC
Pitch Off
⊡ Events/2
(μ/in²)·μanti/10¹² P
80
70
60
50
40
30
20
10
0
1
2
3
4
5
6
7
8
9
10
12
HEIGHT ABOVE FLOOR
ft.

Fig. III-3

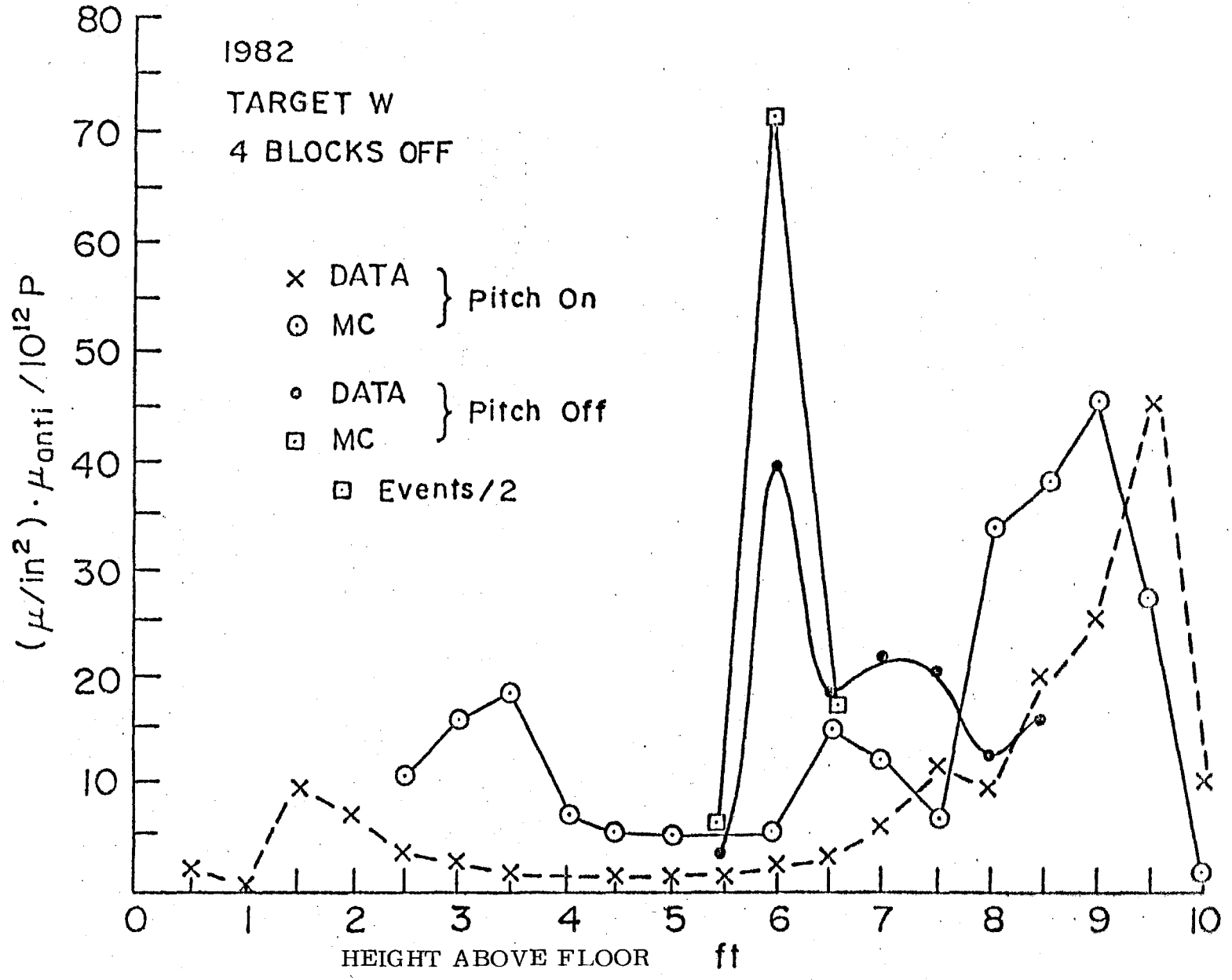
1982
TARGET W
4 BLOCKS OFF
× DATA
⊙ MC
Pitch On
∘ DATA
⊡ MC
Pitch Off
⊡ Events/2
(μ/in²)·μanti/10¹² P
80
70
60
50
40
30
20
10
0
1
2
3
4
5
6
7
8
9
10
HEIGHT ABOVE FLOOR ft

Fig. III-4

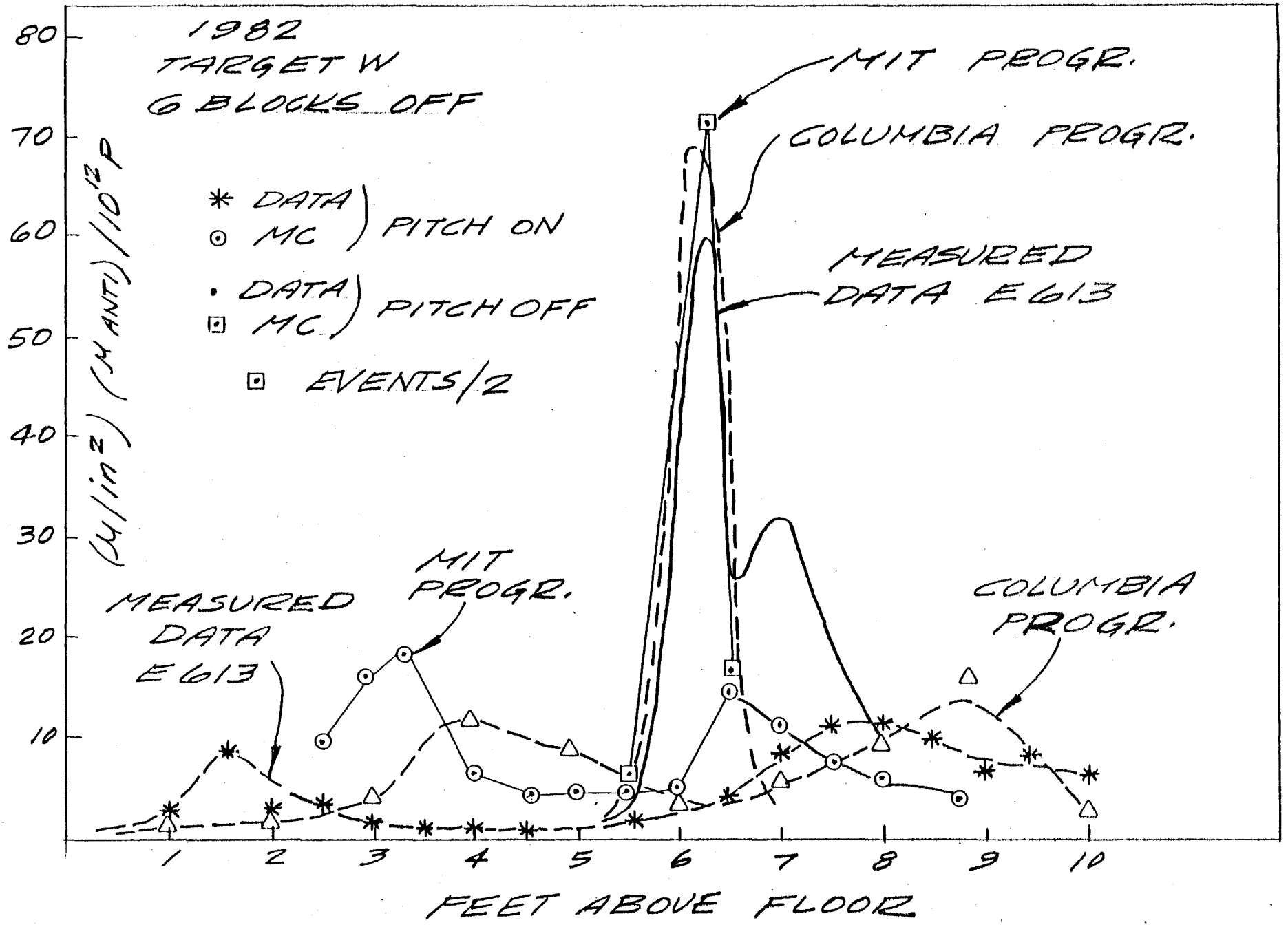
1982
TARGET W
6 BLOCKS OFF
MIT PROGR.
COLUMBIA PROGR.
MEASURED DATA E613
* DATA
⊙ MC
PITCH ON
• DATA
⊡ MC
PITCH OFF
⊡ EVENTS/2
(μ/in²) (μ ANTI)/10¹² P
MEASURED DATA E613
MIT PROGR.
COLUMBIA PROGR.
80
70
60
50
40
30
20
10
1
2
3
4
5
6
7
8
9
10
FEET ABOVE FLOOR

Fig. III-5

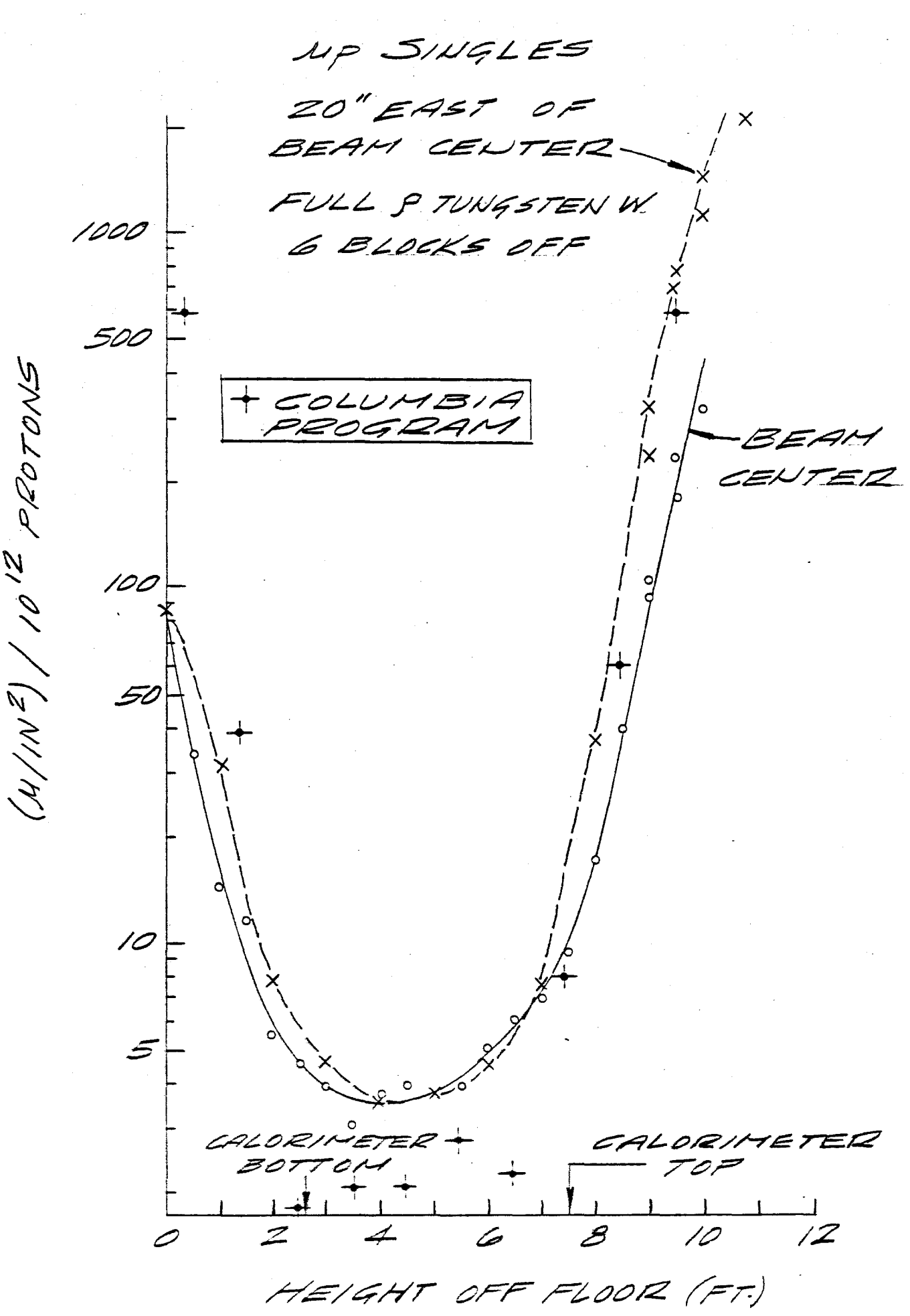
UP SINGLES
20" EAST OF
BEAM CENTER
FULL S TUNGSTEN W.
6 BLOCKS OFF
COLUMBIA
PROGRAM
BEAM
CENTER
CALORIMETER
BOTTOM
CALORIMETER
TOP
1000
500
100
50
10
5
0
2
4
6
8
10
12
(M/IN²) / 10¹² PROTONS
HEIGHT OFF FLOOR (FT.)

Fig. III-6

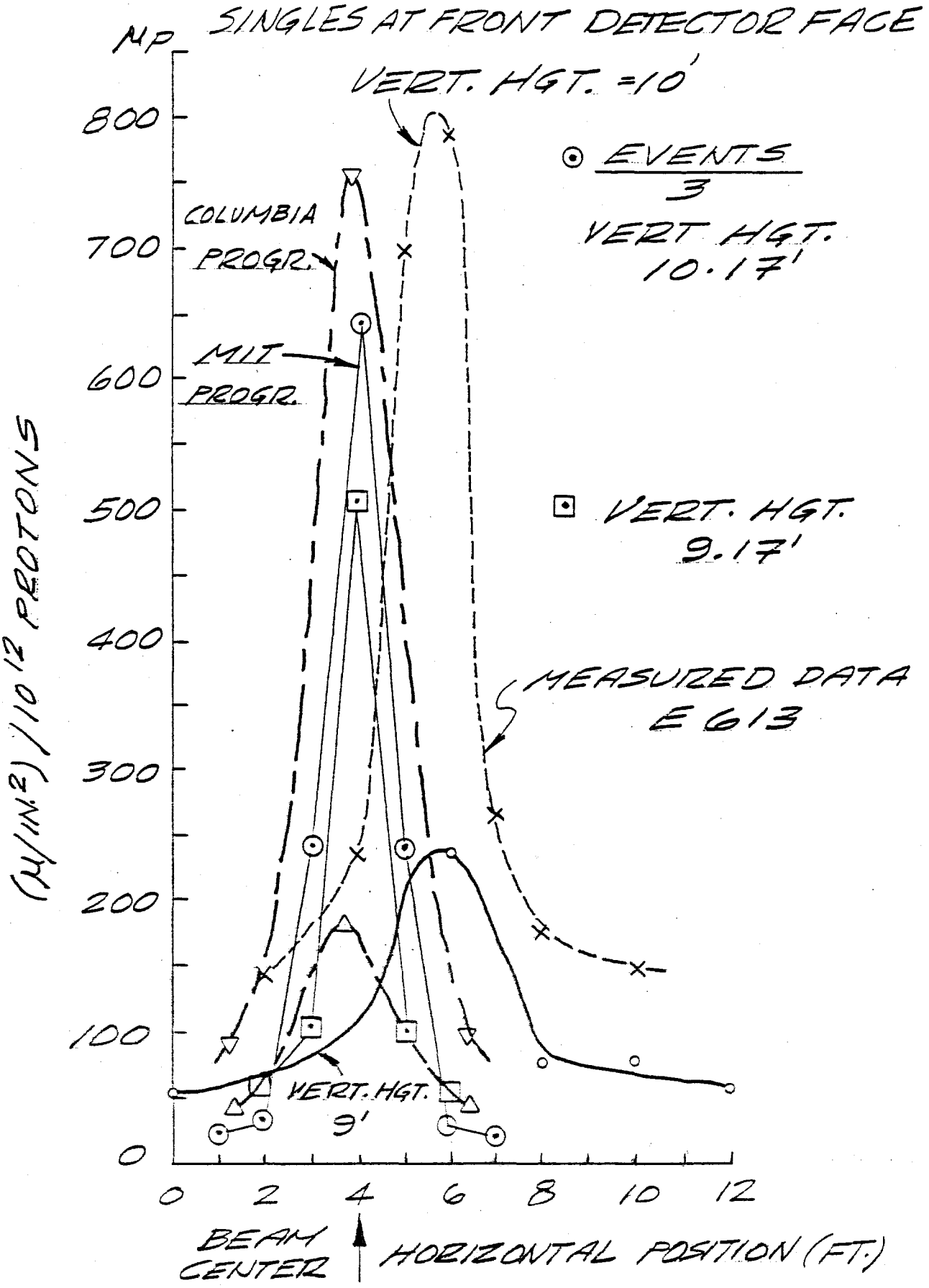
SINGLES AT FRONT DETECTOR FACE
VERT. HGT. =10'
EVENTS
3
VERT HGT.
10.17'
VERT. HGT.
9.17'
COLUMBIA
PROGR.
MIT
PROGR.
MEASURED DATA
E 613
VERT. HGT.
9'
MP
800
700
600
500
400
300
200
100
0
(μ/IN.²) / 10 ¹² PROTONS
0
2
4
6
8
10
12
BEAM
CENTER
HORIZONTAL POSITION (FT.)

Fig. III-7

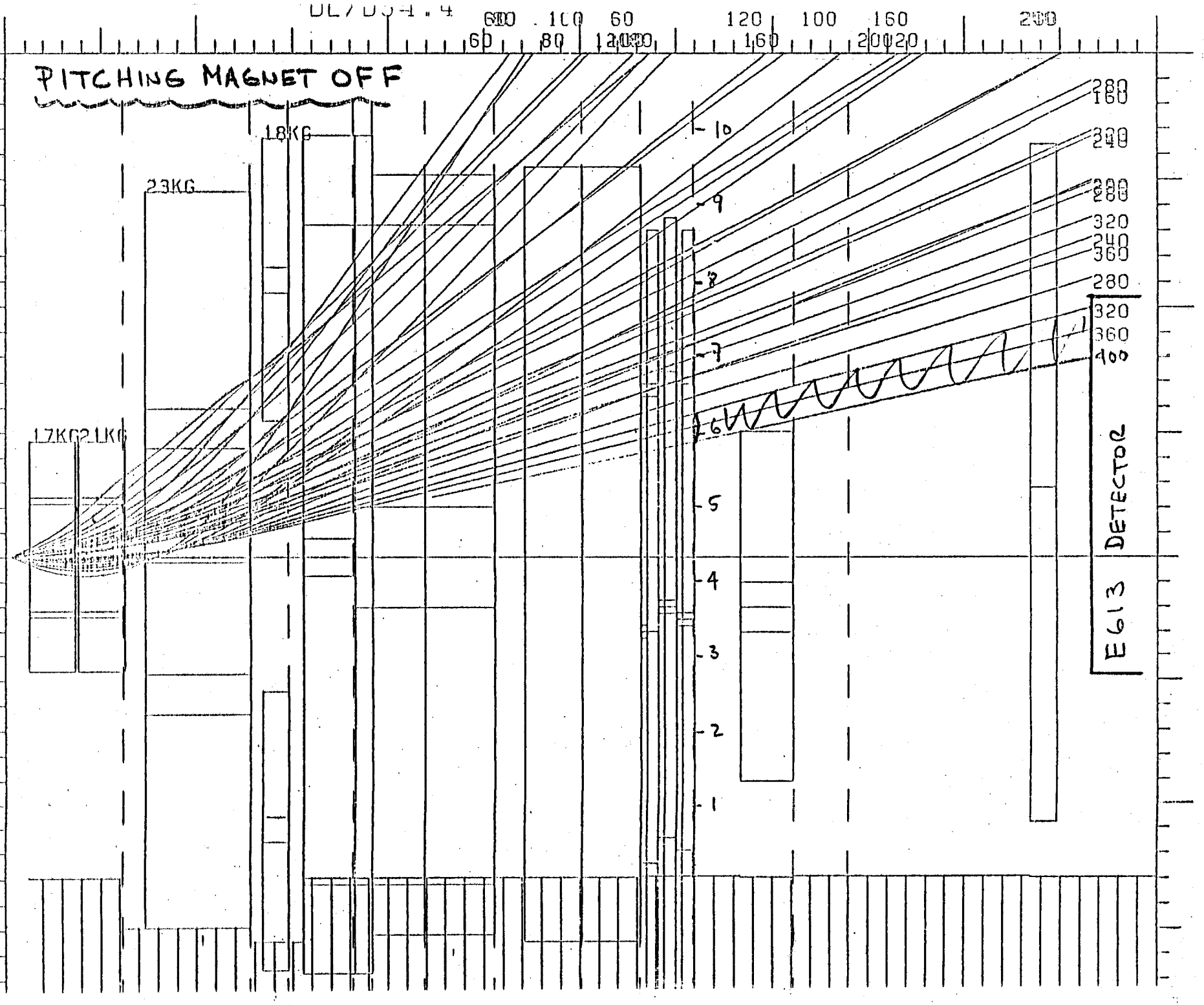
PITCHING MAGNET OFF
1.8KG
2.3KG
1.7KG
2.1KG
E613 DETECTOR
2
1
0
-1
60
80
100
120
160
200
280
320
360
400
240
10
9
8
7
6
5
4
3
2
1

Fig. III-8

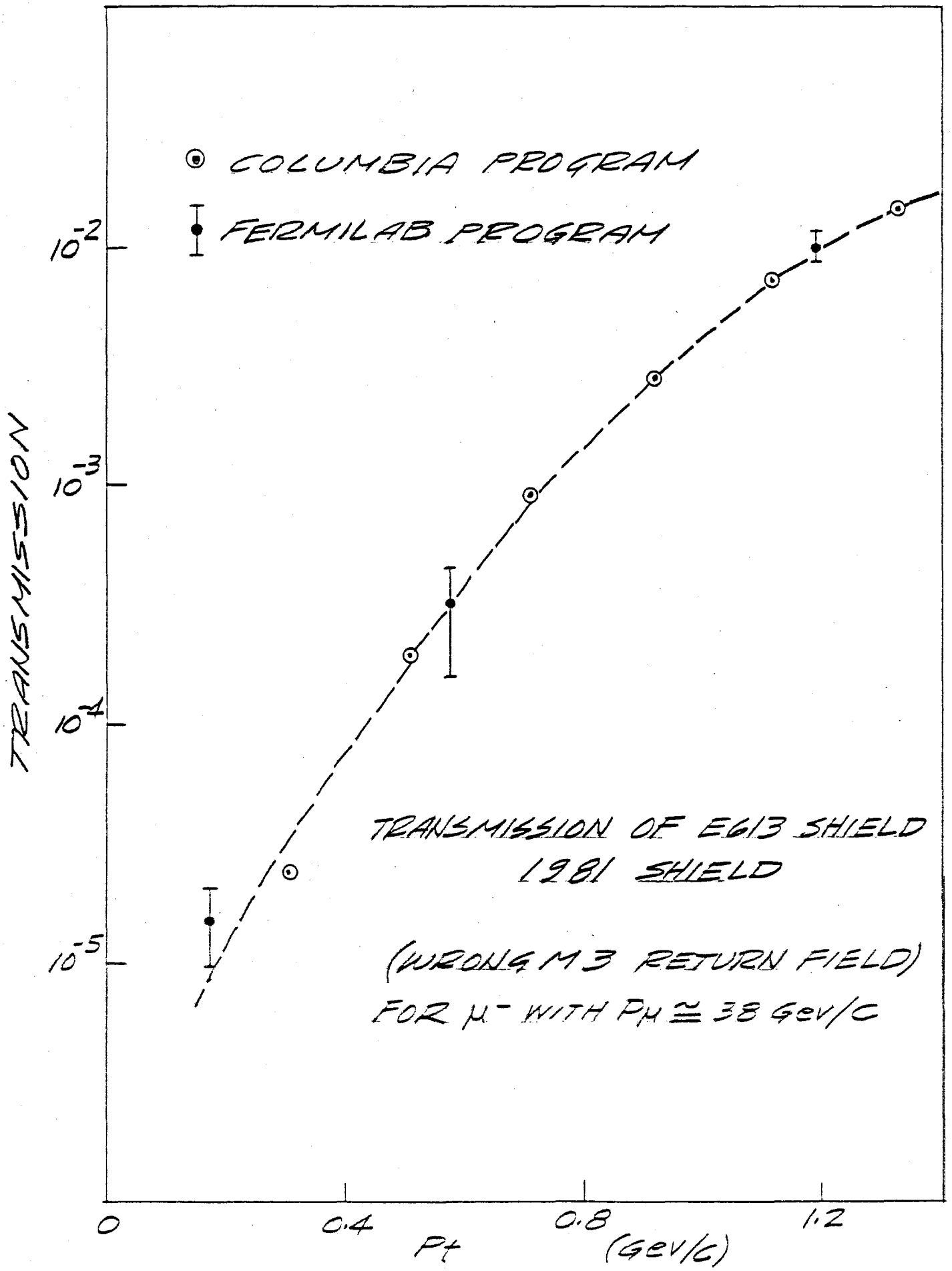
COLUMBIA PROGRAM
FERMILAB PROGRAM
TRANSMISSION
10^{-2}
10^{-3}
10^{-4}
10^{-5}
TRANSMISSION OF E613 SHIELD
1981 SHIELD
(WRONG M3 RETURN FIELD)
FOR μ^- WITH $P_\mu \cong 38$ GeV/C
0
0.4
0.8
1.2
P_t (GeV/c)

Fig. III-9

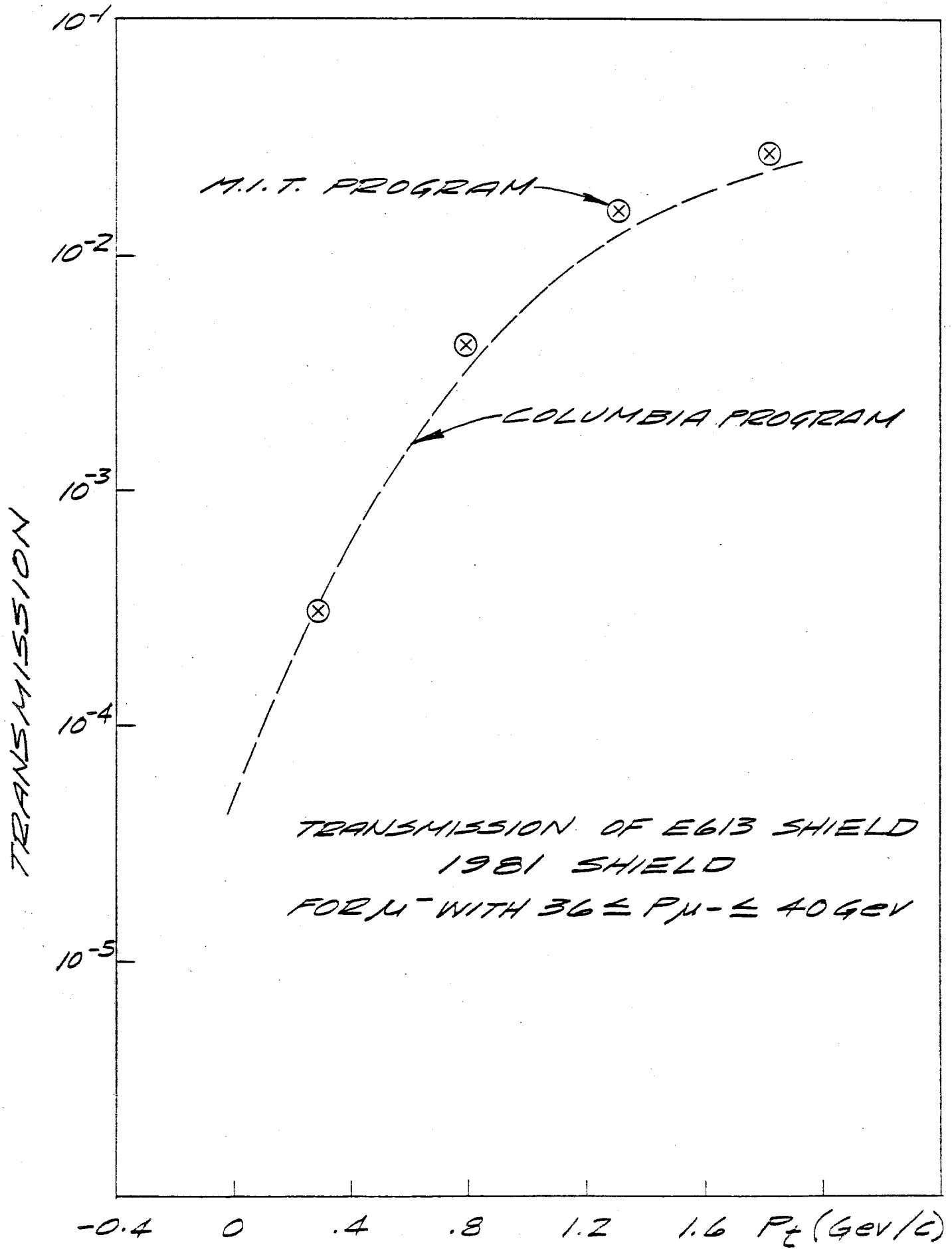
TRANSMISSION
10^{-1}
10^{-2}
10^{-3}
10^{-4}
10^{-5}
M.I.T. PROGRAM
COLUMBIA PROGRAM
TRANSMISSION OF E613 SHIELD
1981 SHIELD
FOR μ^- WITH $36 \leq P_{\mu^-} \leq 40$ GeV
-0.4
0
.4
.8
1.2
1.6
P_t (Gev/c)

Fig. III-10

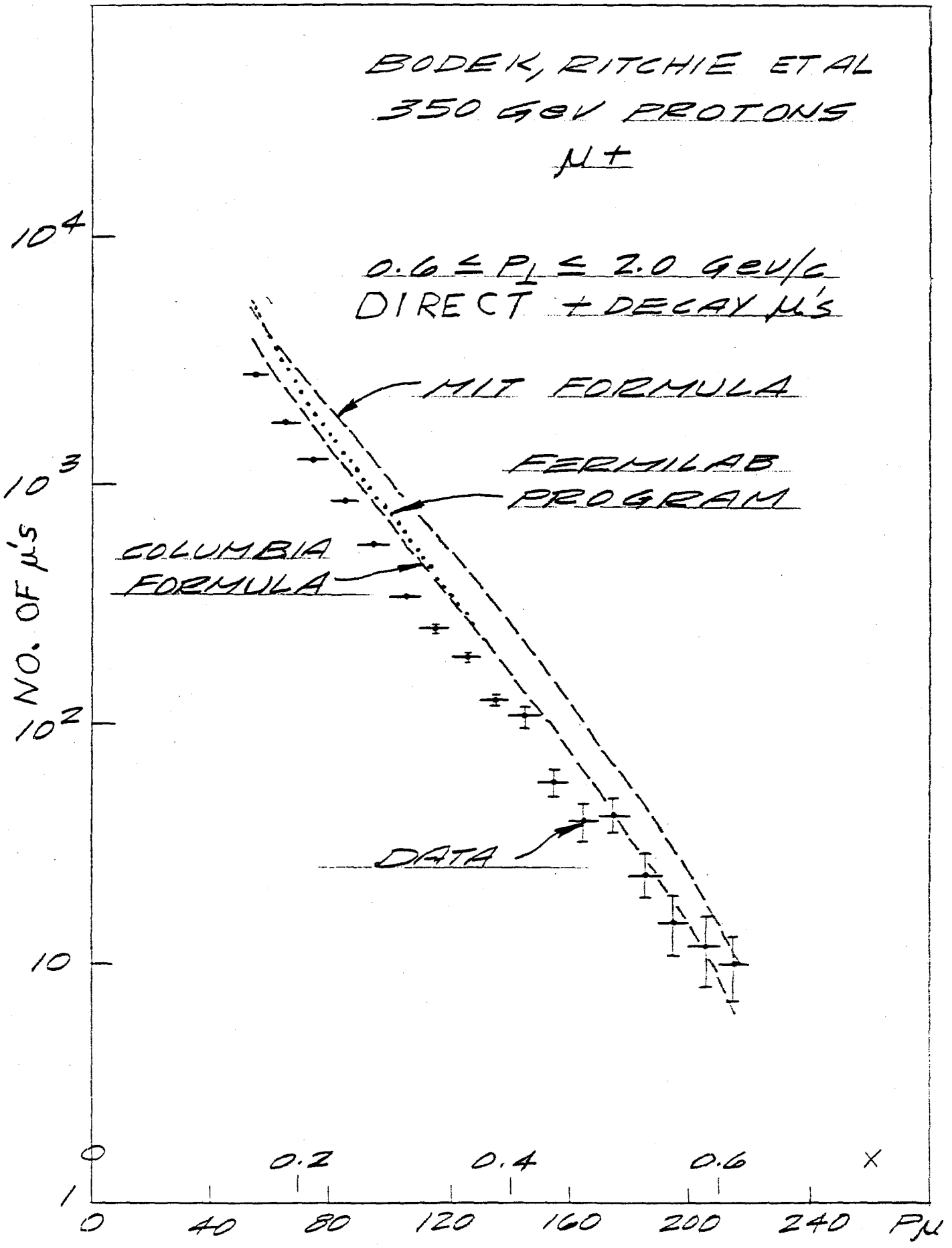
BODEK, RITCHIE ET AL
350 GeV PROTONS
μ+
0.6 ≤ P_L ≤ 2.0 GeV/c
DIRECT + DECAY μ's
MIT FORMULA
FERMILAB PROGRAM
COLUMBIA FORMULA
DATA
NO. OF μ's
10^4
10^3
10^2
10
1
0
0.2
0.4
0.6
X
0
40
80
120
160
200
240
Pμ

Fig. III-11

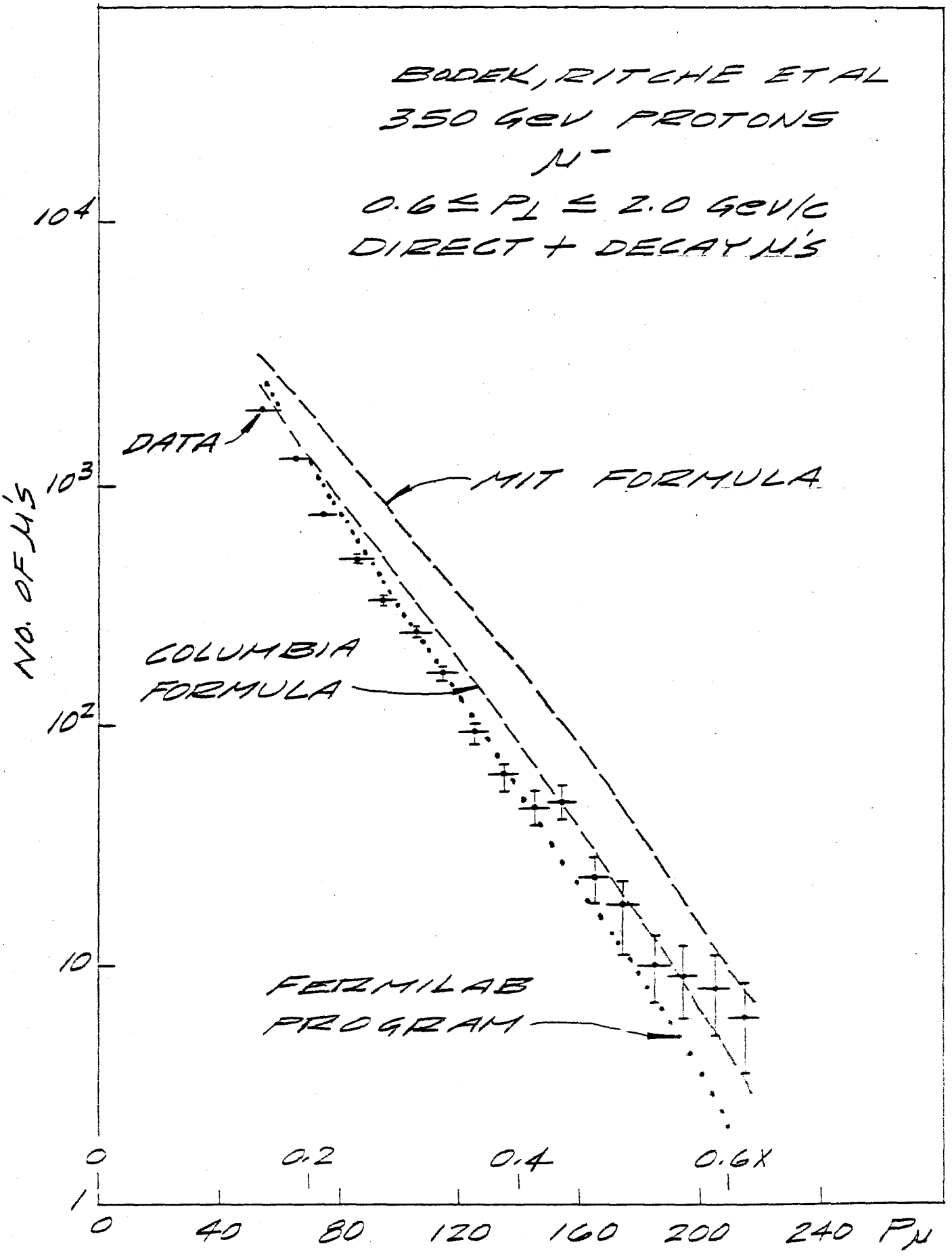
BODEK, RITCHE ET AL
350 GeV PROTONS
μ^-
$0.6 \leq P_L \leq 2.0$ GeV/c
DIRECT + DECAY μ'S
DATA
MIT FORMULA
COLUMBIA FORMULA
FERMILAB PROGRAM
NO. OF μ'S
10^4
10^3
10^2
10
1
0
0.2
0.4
0.6X
0
40
80
120
160
200
240
P_μ

Fig. III-12

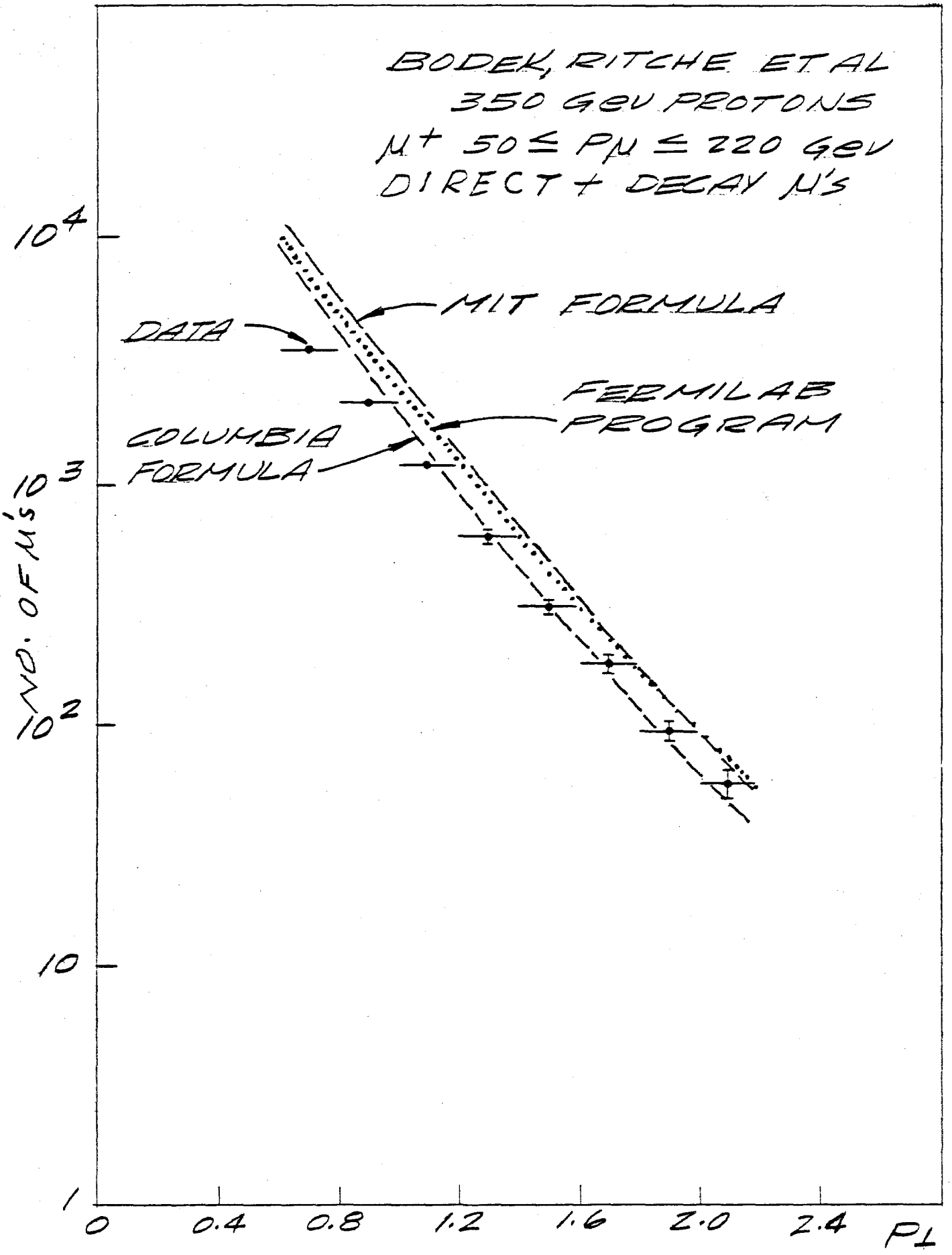
BODEK, RITCHE ET AL
350 GeV PROTONS
μ+ 50 ≤ Pμ ≤ 220 GeV
DIRECT + DECAY μ's
MIT FORMULA
DATA
FERMILAB
PROGRAM
COLUMBIA
FORMULA
NO. OF μ's
10^4
10^3
10^2
10
1
0
0.4
0.8
1.2
1.6
2.0
2.4
P⊥

Fig. III-13

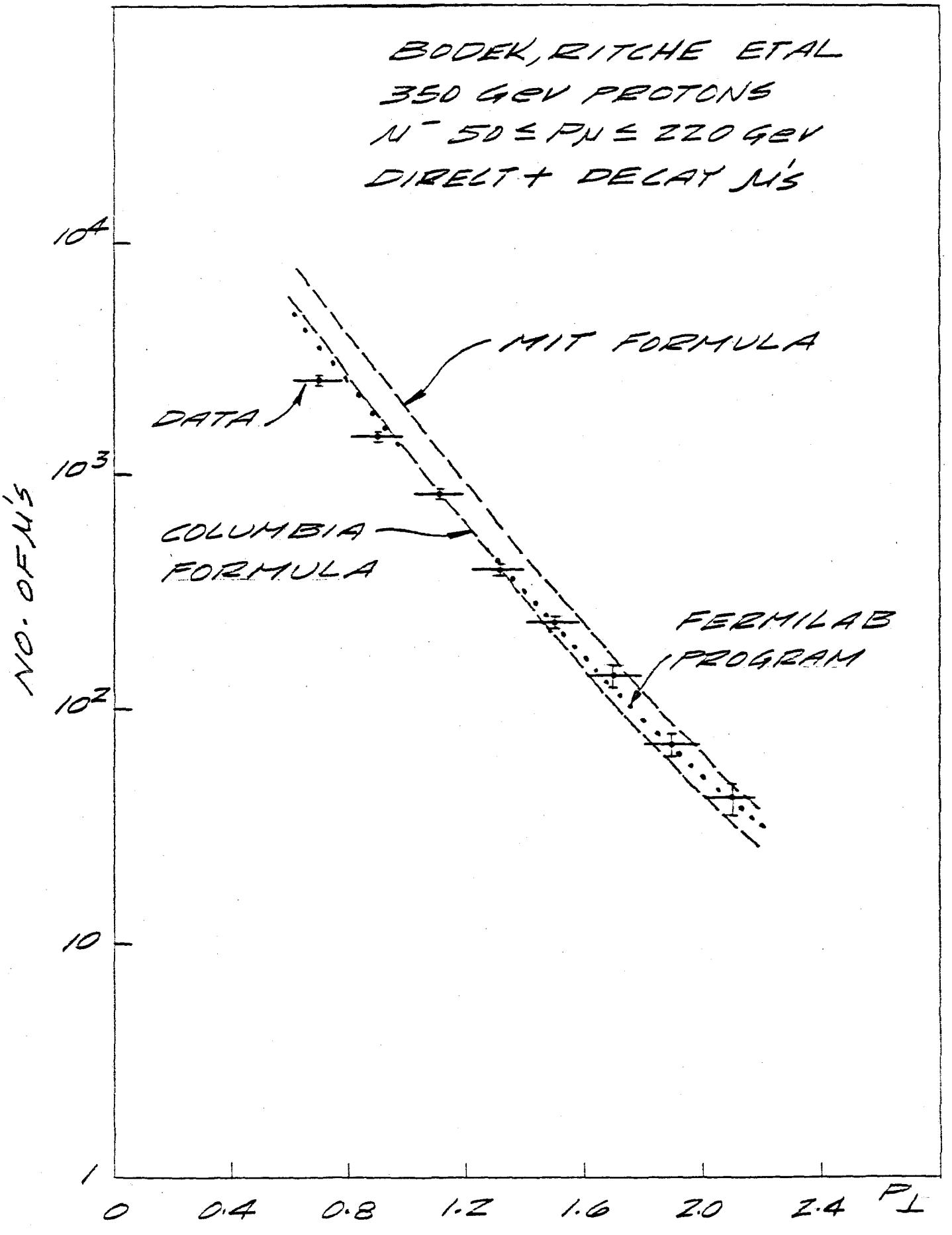
BODEK, RITCHE ETAL
350 GeV PROTONS
μ^- 50 ≤ P_μ ≤ 220 GeV
DIRECT + DECAY μ's
10^4
10^3
10^2
10
1
NO. OF μ's
MIT FORMULA
DATA
COLUMBIA FORMULA
FERMILAB PROGRAM
0
0.4
0.8
1.2
1.6
2.0
2.4
$P_\perp$

Fig. III-14

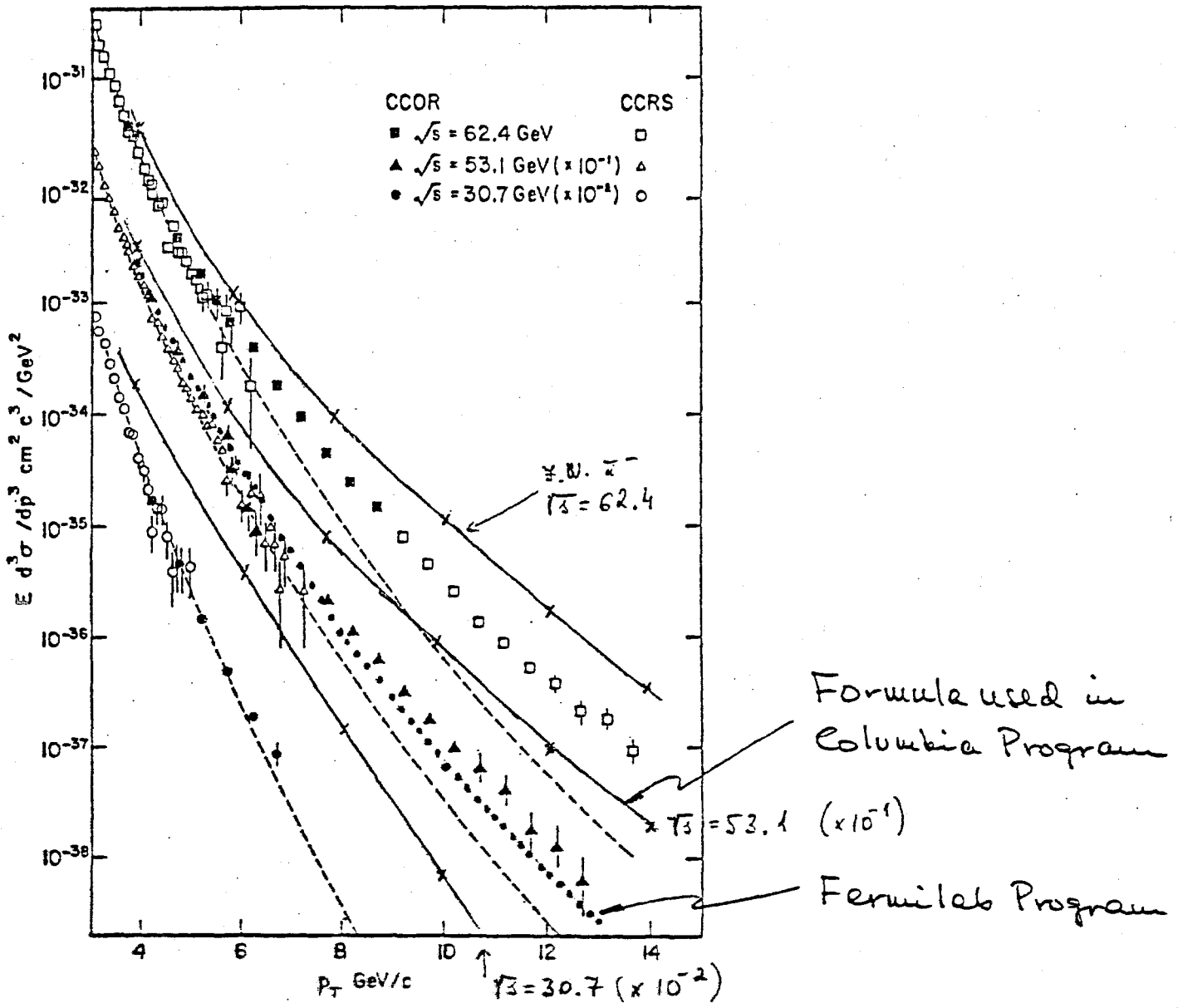
CCOR
CCRS
$\sqrt{s}$ = 62.4 GeV
$\sqrt{s}$ = 53.1 GeV (× 10⁻¹)
$\sqrt{s}$ = 30.7 GeV (× 10⁻²)
E d³σ/dp³ cm² c³/GeV²
P_T GeV/c
π.N. π⁻
√s = 62.4
√s = 53.1 (×10⁻¹)
√s = 30.7 (× 10⁻²)
Formula used in Columbia Program
Fermilab Program

Fig. III-15

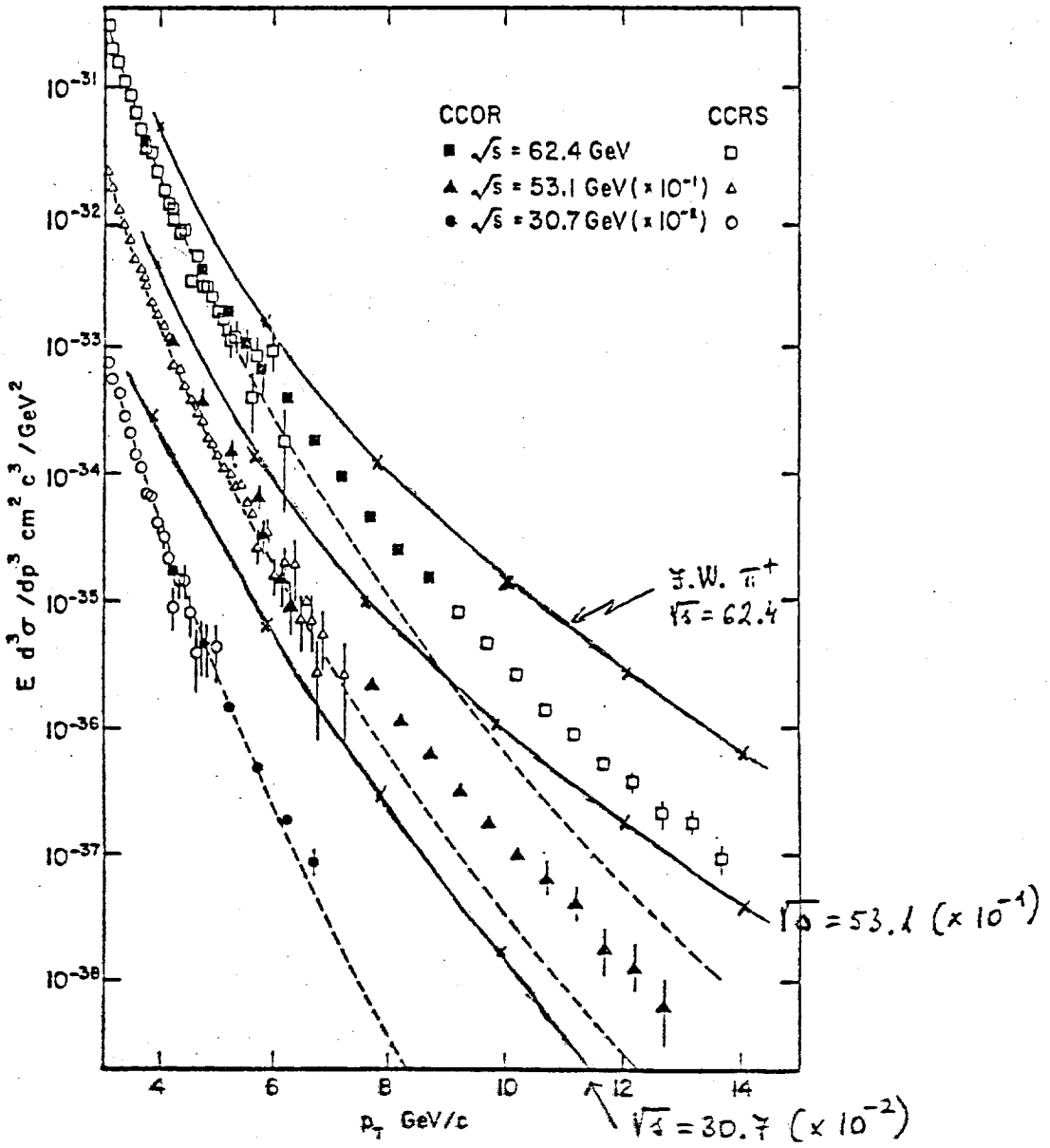
CCOR
CCRS
■ √s = 62.4 GeV □
▲ √s = 53.1 GeV (× 10⁻¹) △
● √s = 30.7 GeV (× 10⁻²) ○
E d³σ/dp³ cm² c³/GeV²
10⁻³¹
10⁻³²
10⁻³³
10⁻³⁴
10⁻³⁵
10⁻³⁶
10⁻³⁷
10⁻³⁸
4
6
8
10
12
14
p_T GeV/c
F.W. π⁺
√s = 62.4
√s = 53.1 (× 10⁻¹)
√s = 30.7 (× 10⁻²)

Fig. III-16

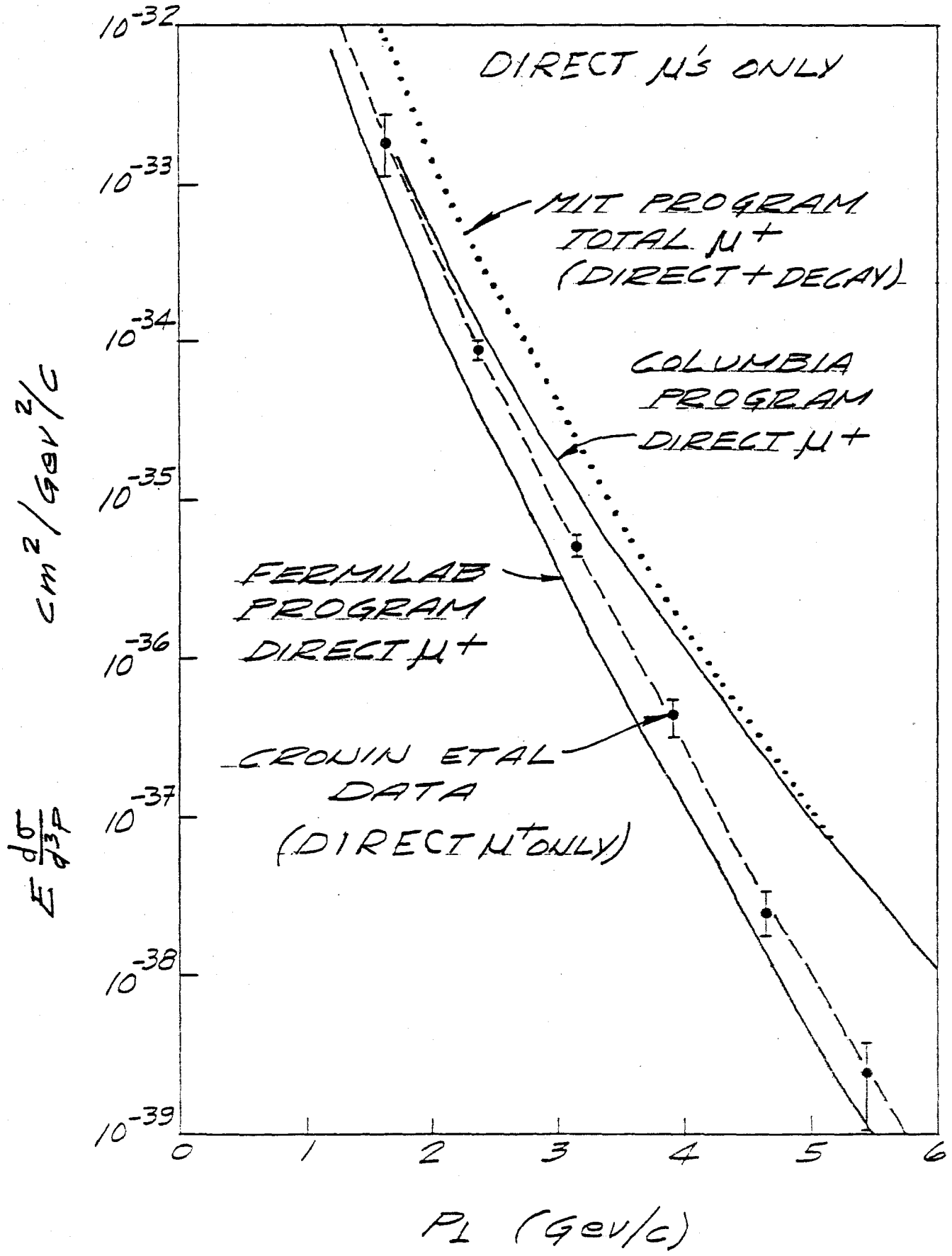
P + NUCLEON → μ+ + ...
COMPARISON WITH DATA BY CRONIN ETAL
DIRECT μ's ONLY
MIT PROGRAM
TOTAL μ+
(DIRECT + DECAY)
COLUMBIA
PROGRAM
DIRECT μ+
FERMILAB
PROGRAM
DIRECT μ+
CRONIN ETAL
DATA
(DIRECT μ+ ONLY)
$E\frac{d\sigma}{d^3p}$ cm²/GeV²/c
10^{-32}
10^{-33}
10^{-34}
10^{-35}
10^{-36}
10^{-37}
10^{-38}
10^{-39}
0
1
2
3
4
5
6
P_L (GeV/c)

Fig. III-17

IV. Muon Spoiler Magnet Design For The Direct Neutral Lepton Facility

To obtain the largest tau-neutrino flux in the detectors, the distance from the target to the detectors must be minimized, for at any reasonable distance the tau-neutrino flux extends beyond the edge of the detectors. In an optimization of the running time versus the cost of the facility, it was decided in 1982 to set the target 160 m upstream of the 15 Foot Bubble Chamber. This optimization was the result of the following contraints and analysis of incremental costs:

1. The 15 Foot Bubble Chamber cannot be moved; thus it is the absolute position of the target which must be selected.

2. A shorter distance between the target and the chamber would increase the event rate (roughly proportional to the distance squared), but the length, and therefore the cost, of the muon spoiler magnet system would grow rapidly, and more than linearly. This effect is illustrated in Figure IV-1, which shows the 500 GeV muon cone emerging from the target, being bent upward by the spoiler magnet system, and barely missing the 15 Foot Bubble Chamber. If the distance from the target to the chamber were shortened, additional magnetic bending would need to be added at the end of the proposed magnets, and this magnet would have to have an even larger air gap than the others.

3. Conversely, a longer distance between the chamber and the target would save spoiler magnet costs, but the cost of building the primary proton beam would increase approximately linearly with distance, as illustrated in Figure IV-2. The bending magnet strings in NE8 and NLA would both have to be increased in length, and the enclosures lengthened. In addition, the data-taking time to get the same number of events would grow as the distance squared, incurring increased operating costs and beam taken away from other experiments.

Following the decision that the distance from the target to the 15 Foot Bubble Chamber should be 160m, the position of the smaller, 1-m Tohoku Chamber was selected to be 58 m from the target, as close as it could be placed without intercepting the muons (See Figure IV-1). Lab F was built for this bubble chamber and the chamber has been installed and operated.

As a design guideline we have required the muon flux in the Tohoku and 15 Foot Bubble Chambers to be less than 10 per 10^{13} interacting protons. This criterion has been satisfied by the use of large magnets to deflect the muons and by locating the detectors at about 58 meters and 160 meters from the target.

General Layout of Area

Figures IV-3 and IV-4 show a layout of the area from the target hall through Lab C, which contains the next-to-last of the neutrino detectors. The principle items downstream of the target point are listed below:

(A) A solid iron magnet, 4 m long, operated at 20 Kg, whose coil can be installed and removed through the target box, called M1.

(B) A second solid iron, 5 m long, 20 Kg magnet, called M2. This magnet cannot be moved once it is installed and surrounded by shielding.

(C) Large air-gap magnets whose purpose is to deflect muons away from the detectors.

(D) The new Tohoku Bubble Chamber and its associated active and passive shield.

(E) Lab E which exists and contains an electronic neutrino detector.

(F) Passive shielding for low energy background radiation.

(G) The 15 Foot Bubble Chamber.

(H) Lab C which exists and contains an electronic detector.

(I) Experiment 635 (not shown).

(Cross sections of the spoiler magnets can be found in Chapter III of this Conceptual Design Report, Figures 4 through 8.)

Here we shall briefly review the general characteristics the first three items. The target box magnet, in addition to bending muons, limits residual activity to less than about 1 R at its downstream face (after zero cooldown time) where electrical and water connections are made. This radiation limit requires that the length of the magnet to be not less than 4.0 m. We have chosen this length because a larger magnet would be impossible to service through the Target Hall. The second magnet, in addition to contributing to the sweeping action on muons, attenuates the neutron flux from the dump target. At the downstream face of the magnet there is a tolerably low neutron flux such that the bubble chambers can operate successfully at 58 and 160 m respectively.

The design of the remaining large magnets for deflection of muons out of the detectors has demanded an exhaustive and extensive study. The primary beam energy was assumed to be 1000 GeV.

The number of ≥ 800 GeV muons produced in a target is adequately low that they may be permitted to strike detectors. To sweep out 800 GeV/c momenta imposes a lower limit to the integral magnetic field bending power. This corresponds to about 600 Kg-meters, including the two solid-iron magnets mentioned above. The transverse dimensions of the magnetic field must be such that all muons of greater than about 40 GeV/c and $P_t \leq 10$ GeV/c must also be swept out of line of the detectors otherwise the fluxes are unacceptably high.

Extensive studies, involving many iterations through system design followed by Monte-Carlo evaluation, led to the following necessary properties for the remaining magnets (following M1 and M2):

1. They must be air-gap magnets, in order to avoid any further deep-inelastic scattering or trident production from the high-energy muons passing through the gap.

2. In order to sweep out the high-P_t muons which first get bent back towards $P_t = 0$, the total field integral of the system (including M1 and M2) must be 660 Kg-m.

3. These additional magnets must be able to sweep away the wrong-sign muons produced by trident production in M1 and M2. In satisfying this requirement, a very subtle effect was discovered: a wrong-sign muon of medium or high energy near the lower edge of the field region needs to see either the full field (in order to be kicked up to above the detectors) or no field at all (in order to continue to drift down to below the detectors). This led to the requirement that the field fall from 20 Kg to 0 as quickly as is practical, which led to vertically "thin" coil packages and rather high current densities.

4. After the field falls abruptly to zero, the field must remain near zero for a considerable distance in order that medium-energy (25 to 70 GeV) muons are not bent back towards the detectors in the return leg of the steel, but rather continue on into the dirt. This effect is illustrated for 60 GeV muons in Figure IV-5. The result is that these final magnets are very deep C-magnets, with the bottom return leg several meters below the air gap.

5. The "band-pass" energy is that energy range in which muons swept down by M1 and M2 do enter the return legs of the final magnets and are swept back towards the detectors. This energy region has been chosen to be 20±5 GeV, which is low enough that these muons can be ranged out by concrete shielding judiciously placed just above the return leg (see Figure IV-6 for an illustration at 25 GeV), which these muons intercept after leaving the iron return leg.

6. Because of criterion (4) above, these magnets involve an unusual amount of steel, mostly contained in the tall vertical side legs. Steel, not copper coils, dominate the cost of magnets. Therefore it is desirable to push the steel well into saturation with extra copper and amp-turns, in order to keep the steel as short as is feasible. On the other hand, pushing to too high a field would violate criterion (3) above, and also increases power and copper costs much faster than linearly with field. A field of 20 Kg was found to be an approximate optimization.

Figure IV-3 shows a layout of the six magnets required in this design. A preliminary engineering design of this system has been made by R. Fast of Research services (see below). The magnetic field profiles of the magnets have been calculated and included in the programs which calculate the muon fluxes. The D.C. power requirement is 4.1 MW. However, it has been shown that the magnets can be pulsed to match the repetition rate of the Tevatron and thereby reduce power consumption to about 1.1 MW.

When the proton beam is targeted at non-zero angle relative to the detector axis, it is necessary to move the air-gap magnets sideways to align the air-gap region with the region of high muon flux. Under these conditions, the muon rate into any detector for production angles in the range 0 - 40mr is acceptably low as defined earlier.

Muon Fluxes From The Dump

Muon fluxes in the Tohoku and 15 Foot Bubble Chambers have been calculated independently by the three programs described earlier. These fluxes are for the case of a full density tungsten target and include prompt and non-prompt muon production sources. Final results are shown in the attached table. The calculations refer to:

I. Columbia

II. Hawaii-Fermilab

III. MIT

The results of the different calculations are in good agreement with each other as they were in the case of the E-613 shield calculation. It can be seen that no more than a few muons per 10^{13} protons at 1000 GeV are expected in either of the bubble chambers.

Table IV-1

Muons per 10^{13} proton in each of the two bubble chambers from three physical processes and the three computer programs, for 1000 GeV incident protons and spoiler magnets M1 through M6.

		1m B. C. CALCULATION			15 Foot B. C. CALCULATION		
		I*	II*	III*	I	II	III
Coulomb Scattering	μ^+	0.3	0.2	0.5	<0.1	<0.1	<0.1
	μ^-	0.3	0.5	0.5	<0.1	<0.1	<0.1
Deep Inelastic Scattering	μ^+	0.2	<0.1	<0.1	<0.1	<0.1	<0.1
	μ^-	<0.1	<0.1	0.5	0.1	0.1	1.0
Trident Production	μ^+	0.5	0.1	1.5	<0.1	0.7	0.2
	μ^-	0.2	0.1	0.5	0.5	0.2	0.5
Total		1.6	1.1	3.6	1.0	1.3	2.0

* I = Columbia

II = Fermilab

III = MIT

Some general comments on muons from the various sources is of interest.

i. Coulomb Contribution

a. Muons in the band pass energy.
This source may be the most serious if the design is not done properly because of the potentially very high intensity. In the present designs, the band pass energy is around 20 GeV which is sufficiently low so that the muons can be absorbed in the passive shield inside the magnets. There is no resulting muon contribution from this source.

b. Muons with Threshold Energy
Other than the muons in the band pass, there are muons which barely escape out of the dump with energy around and less than 1 GeV. These low energy muons may scatter with a very large angle and hit the chambers. Although the muons can be absorbed in the passive shield in front of the chambers, it is safer not to have them in the first place. To eliminate the problem, a small magnet (called spoiler) with low field could be placed so that it kicks away the low energy muons that just emerge from the absorber in the magnet M2. There is also no resulting muon background contribution from this source.

c. Muons get caught in the fringe field.
As shown below, the field of the C-magnets extends beyond the coil, unlike in a solid iron magnet, in which there is a sharp cut off of magnetic field. Because the field around the coil is neither strong nor weak there are muons with energy of around 40 GeV and vertical P_t of around ±5 GeV which get caught and bent back toward the detectors. The muon background to the 1m Bubble Chamber from this process is ~2. There is no contribution to the 15 Foot Bubble Chamber from this process.

ii. Muons Scattered Deep Inelastically.

Since both systems are designed so that high energy muons with high intensity do not pass through much material in the dump, the design has no serious problems from this source.

iii. Trident Production.

Any trident produced inside a magnet field is potentially dangerous. As mentioned earlier, this is the reason for air-gap magnets. The major source of tridents is the pole face of the magnets which are hit by high P_t muons. There are two muons in the background in the 1m chamber. Another source of tridents for the 15 Foot Bubble Chamber is the magnet yoke of the 1m chamber. One

sign of muon produced in the magnet bends toward the 15 Foot Bubble Chamber, and this gives about five muons as background. Modification of the 1m Bubble Chamber magnet yoke has been completed. A slot in the magnet was made so that high intensity muons do not interact. With the slot the background gets better by a factor of six so that there is less than one muon in the 15 Foot Bubble Chamber Another reason for the slot is to reduce the background in the downstream detectors of the 1-m Bubble Chamber. It is found that without the slot there are about 20 muons in CRISIS from tridents produced in the magnet. With this slot the number drops by about a factor of five.

Magnet Requirements

Bo = central field = 2.0 T

ΔB = variation of central field = ± 0.1 T

$\int Bdl$ = 48 T-m (1575 kG-ft)

$(-B_x)_{max}$ = maximum value of reversed horizontal field component outside aperture ("fringe field"):

0.1 T above coil

0.2 T below coil

$B_x(y)$ should drop quickly outside the aperture

The above tolerances on ΔB and fringe field are very easy to achieve and put very little demands on the precision of the assembly and steel quality.

A C-magnet style with racetrack coils was chosen to avoid tall, narrow magnets. In order to reduce the power requirements, a pulsed current design was considered.

Calculations

The magnetostatic problem was solved in two dimensions, the x-y plane, using the program LINDA. The program calculates horizontal and vertical field components as a function of position in the x,y plane of longitudinal symmetry, B_x (x,y,0) and B_y (x,y,0). The value of the horizontal component on the mid-plane, B_x (0,y,0), for each of the four magnets is given in Table IV-2.

Calculations in the y,z plane, giving B_y (0,y,z) and B_z (0,y,z), will be done as part of the final design.

In the calculations the coils were sized such that the current density was approximately 2900A/in^2 (450 A/cm^2). At current densities much higher than this power requirements become large and pulsing more difficult. Lower current densities, with larger coils, result in the field dropping too slowly outside the aperture.

The coil inductances were calculated from $L = N\phi/I$ = flux linkages per amp. The DC power was obtained from $PDC = \rho J^2 V$ (ρ = resistivity, V = volume of copper in coil) and the resistance $R = PDC/I^2$.

Coil and Iron Parameters

The parameters of magnets which were found by S. Oh to be satisfactory are given in Table II, Chapter III of this Conceptual Design Report.

Pulsing the Magnets

The magnets must be pulsed to reduce the AC power requirements. They will be ramped from some low current, a few hundred amperes, to 5 kA and back down once per one minute Tevatron beam pulse.

Preliminary calculations, using the parameters of Table II, show that the magnet circuits can be charged and discharged in one minute, reducing the power dissipation to about one third of the DC value.

Table IV-2

Mid Plane Field Distribution

Vertical Position (cm)	B_x in tesla for magnets M3	M4	M5	M6
400	-0.007	-0.010	-0.010	-0.012
350	-0.009	-0.013	-0.013	-0.015
300	-0.012	-0.018	-0.017	-0.020
250	-0.016	-0.023	-0.022	-0.026
200	-0.020	-0.027	-0.022	-0.030
150	-0.003	-0.026	-0.015	-0.021
100	0.440	0.961	1.209	0.958
50	1.927	1.944	1.951	1.944
0	2.000	2.000	2.000	2.000
-50	1.928	1.947	1.944	1.947
-100	0.425	0.953	1.214	0.947
-150	-0.038	-0.018	0.050	-0.032
-200	-0.051	-0.075	-0.072	-0.092
-250	-0.039	-0.066	-0.069	-0.082
-300	Iron	-0.052	-0.058	-0.069
-350	Iron	-0.034	-0.048	-0.058
-400	Iron	Iron	-0.036	-0.048
-450	Iron	Iron	-0.015	-0.037
-500	Iron	Iron	Iron	-0.022

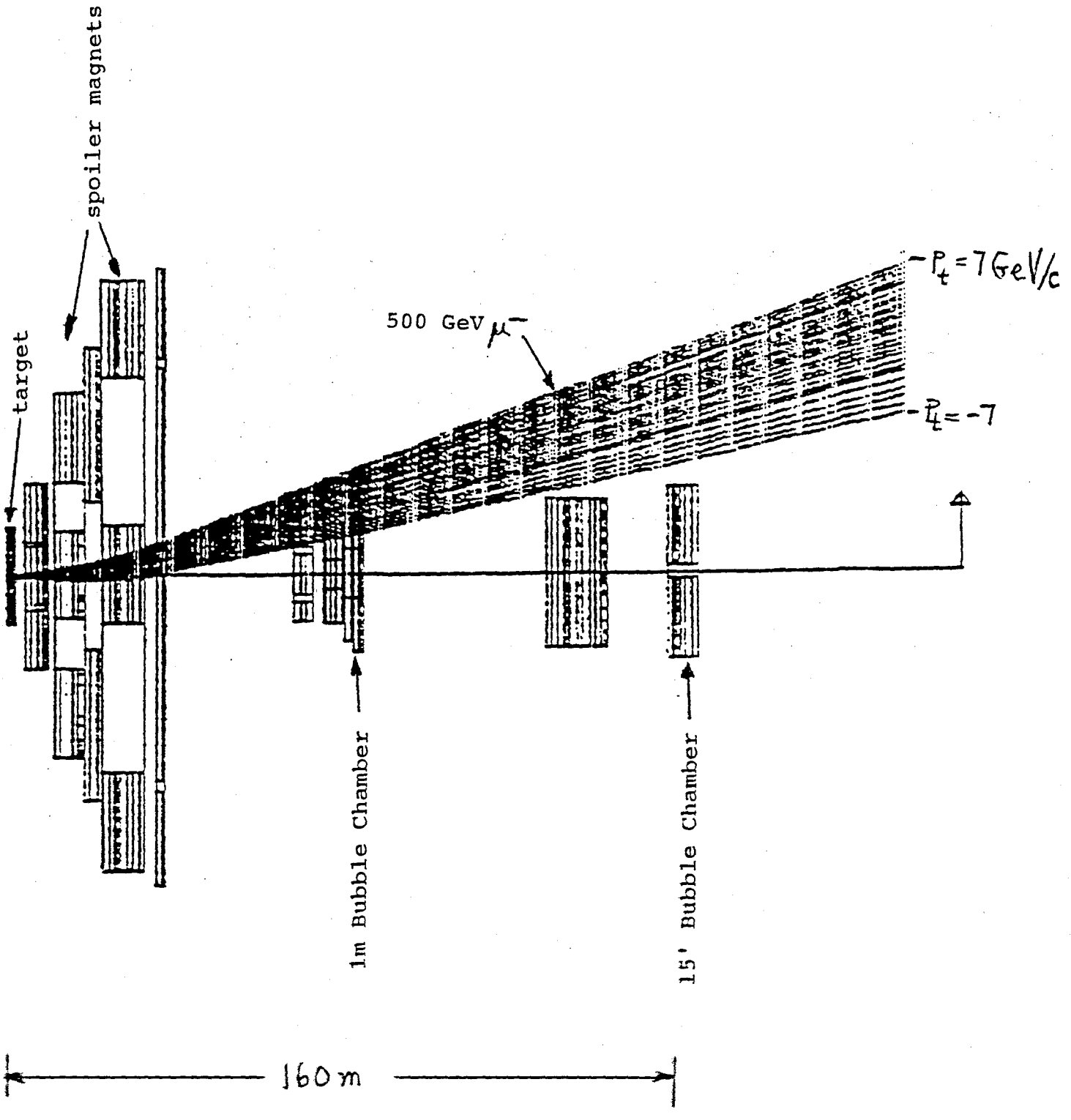
spoiler magnets
target
500 GeV μ^-
$P_t = 7$ GeV/c
$P_t = -7$
1m Bubble Chamber
15' Bubble Chamber
160 m

Fig. IV-1

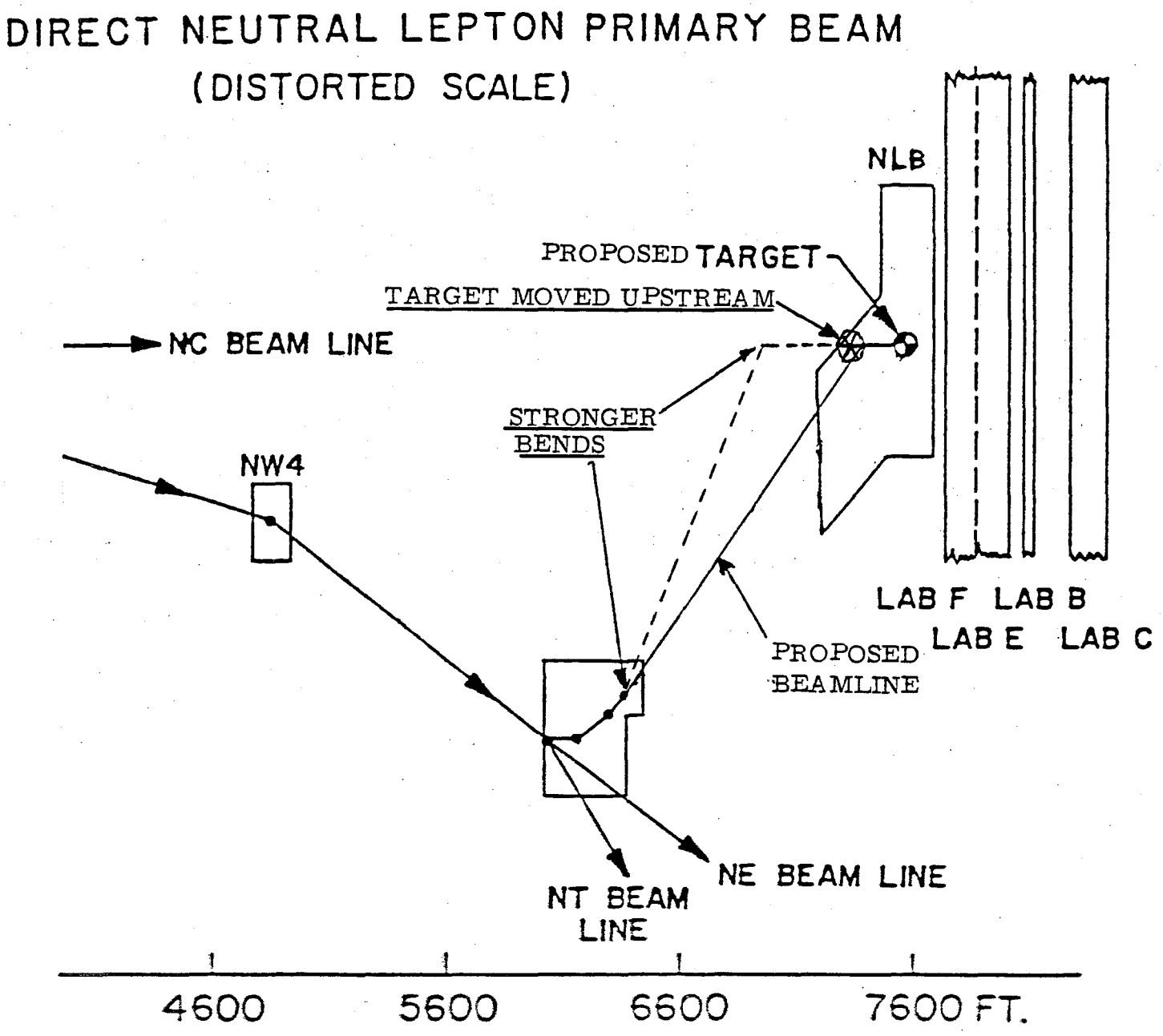
DIRECT NEUTRAL LEPTON PRIMARY BEAM
(DISTORTED SCALE)
NLB
PROPOSED TARGET
TARGET MOVED UPSTREAM
NC BEAM LINE
STRONGER BENDS
NW4
LAB F
LAB B
LAB E
LAB C
PROPOSED BEAMLINE
NE BEAM LINE
NT BEAM LINE
4600
5600
6600
7600 FT.

Fig. IV-2

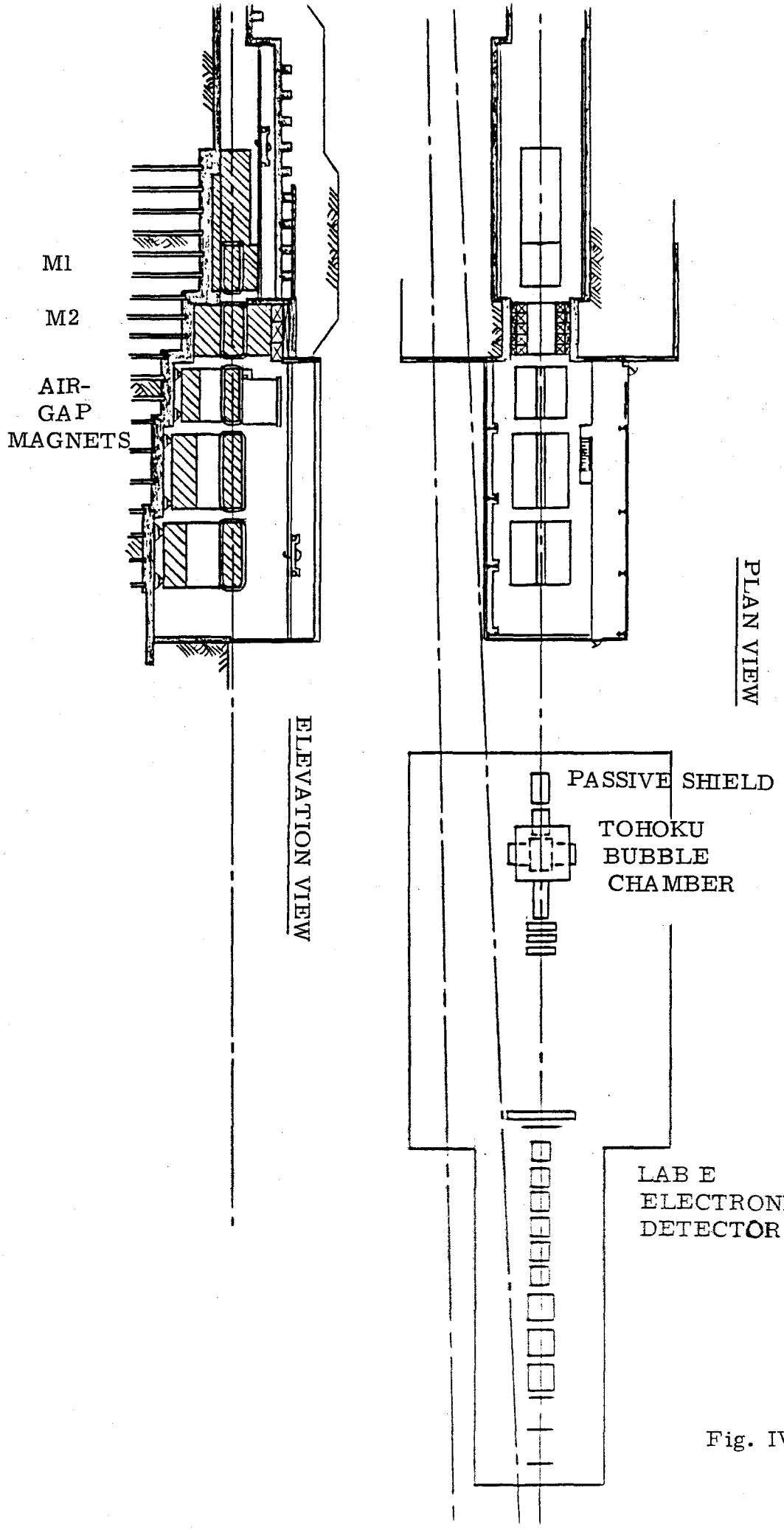
M1
M2
AIR-
GAP
MAGNETS
ELEVATION VIEW
PLAN VIEW
PASSIVE SHIELD
TOHOKU
BUBBLE
CHAMBER
LAB E
ELECTRONIC
DETECTOR

Fig. IV-3

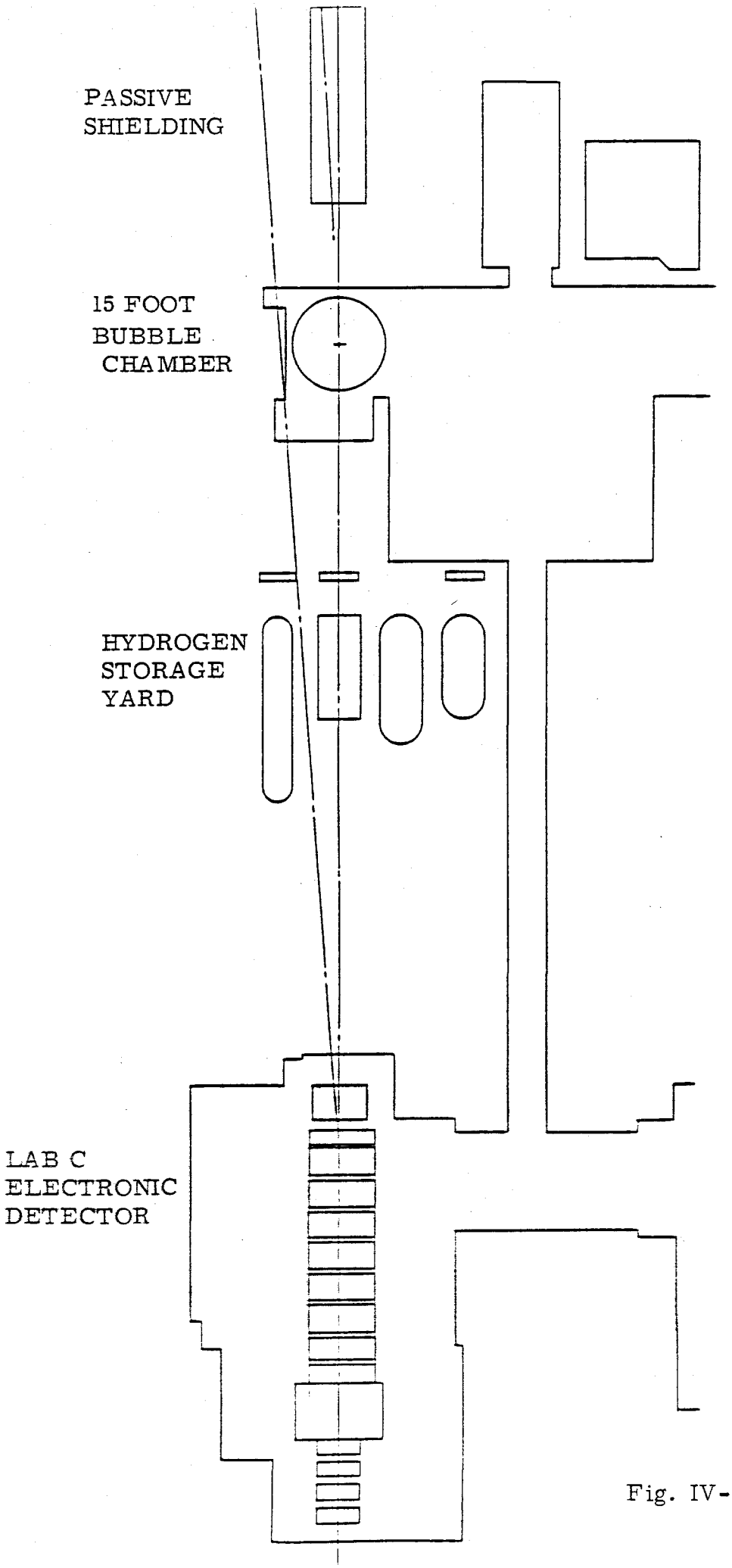
PASSIVE
SHIELDING
15 FOOT
BUBBLE
CHAMBER
HYDROGEN
STORAGE
YARD
LAB C
ELECTRONIC
DETECTOR

Fig. IV-4

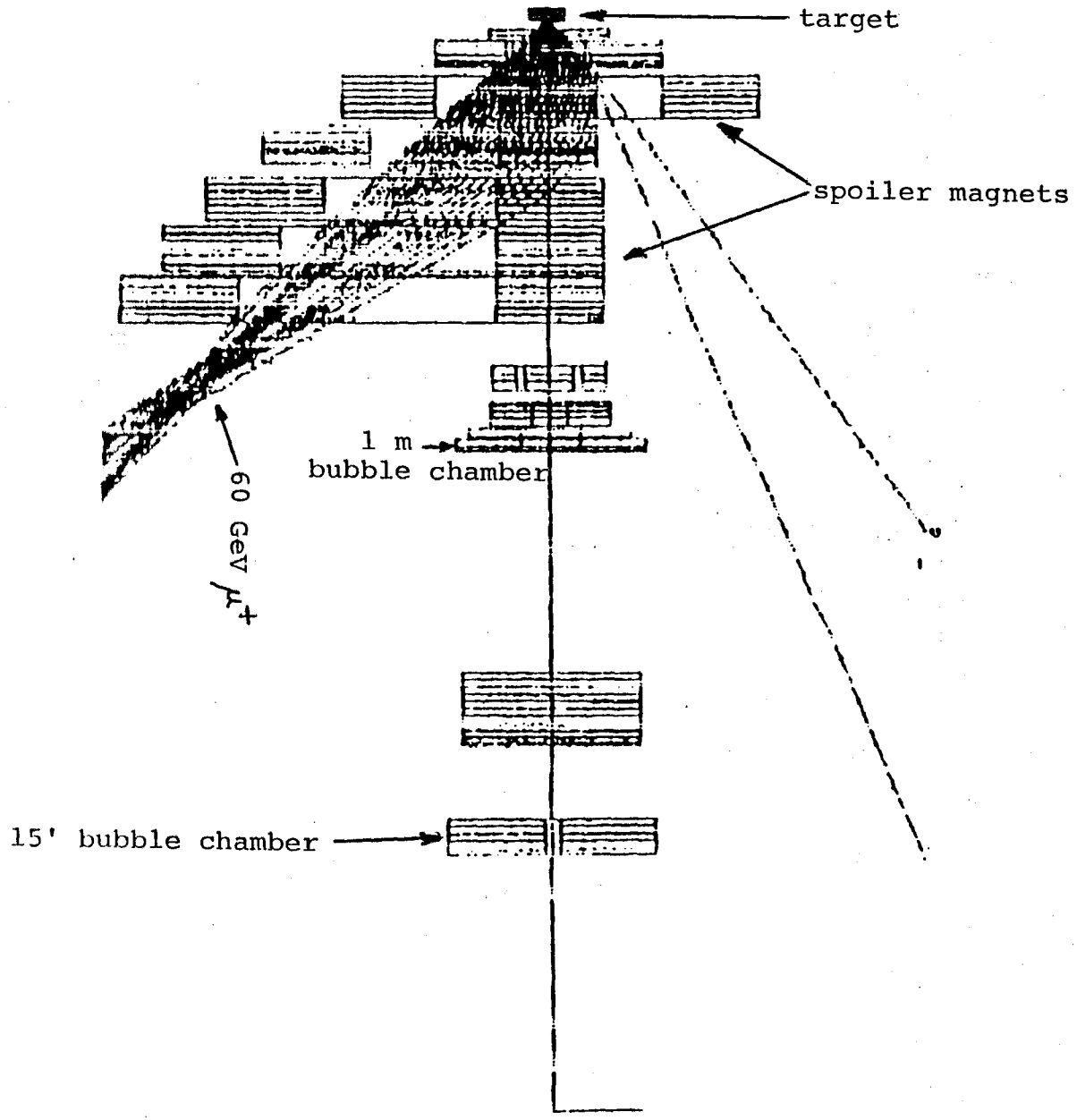
target
spoiler magnets
1 m
bubble chamber
60 GeV μ^+
15' bubble chamber

Fig. IV-5

25Gev

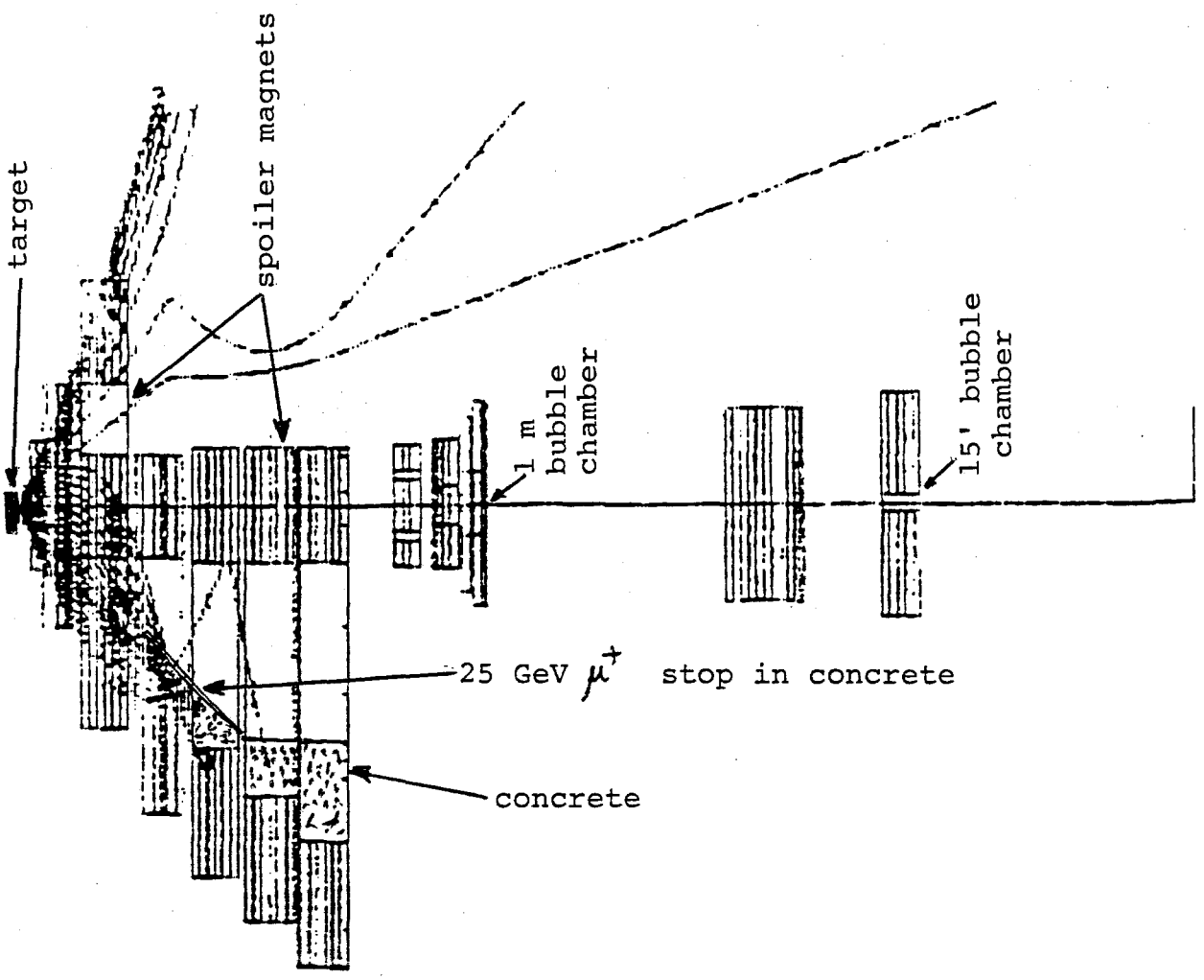

Fig. IV-6

V. Redesign of the Spoiler System for 900 GeV Incident Protons

Motivation and Consequences

Some number of people believe that the fixed target program at Fermilab will never operate at an energy higher than 900 GeV, or at least not at high intensity, because of extraction losses. Should this belief prove to be true, then a 900 GeV design for the Direct Neutral Lepton Facility is fully justified. There is not even any physics lost.

Therefore, the proponents of the Direct Neutral Lepton Facility undertook, in the summer of 1984, to redesign the muon spoiler system for 900 GeV, knowing that shortening the length of the spoiler magnet system saves expensive magnets in a manner in which the total spoiler magnet costs drop faster than linearly with momentum. A redesign has been completed, but not as fully optimized as was the 1000 GeV design.

The beamline has also been designed for 900 GeV, but the capability of pushing it to 1000 GeV by the addition of more power supplies has been preserved.

Should the machine ever extract 1000 GeV protons, then one has two choices. If the muon background at 900 GeV has been small, one can upgrade the beamline and try 1000 GeV. Alternately, one can extract 900 GeV protons to the dump on a "front porch" in the accelerator ramp, and then accelerate the remainder of the protons to 1000 GeV for the remaining users. This latter option may even be attractive to the accelerator operations, if the intensity at 1000 GeV is limited by extraction losses.

The flux of tau neutrinos may go down as much as a factor of two between 1000 GeV and 900 GeV (Morfin suggests only 20% in TM-1275), which may sound like a loss of physics. However, this potential loss is more than offset by the greater proton intensity and accelerator reliability available at 900 GeV.

A Particular Redesign

Hand calculations indicated that removing M6 from the original 1000 GeV design would exactly satisfy the needs of a 900 GeV system. Deleting this magnet would save 19% of the total costs of the spoiler system (based on 1982 estimates), or $2.0M (based on the appropriate fraction of the 1985 cost estimate for M1-M5).

This particular redesign has been run through one of the three Monte Carlo programs by Seog Oh at Duke University using the MIT program. This program gave the highest muon rates in two bubble chambers at 1000 GeV and is therefore regarded as the most pessimistic, or conservative of the three programs.

The results are that the contributions from deep inelastic muon scattering and trident production are the same as shown in Table IV-1, but the contributions from Coulomb scattering have increased to about two in the Tohoku Chamber (total visible volume) and to about 0.5 in the fiducial volume of the 15 Foot Chamber, with another 3.0 between the fiducial volume and the camera lenses. This increase is still within the design criterion of less than 10 muons per 10^{13} protons.

The Monte Carlo program data for the number of muons of all momenta as a function of distance above (or below) each chamber are shown in Figure V-1 and 2, for both the 900 GeV design (M1-M5) and the 1000 GeV design (M1-M6). It should be noted that the source of the few muons which enter the bubble chambers is high P_t muons. The MIT program, as noted in Section III of this appendix, is known to overestimate high P_t muons by a factor five to 10, compared with 300 GeV data and ISR data. Therefore, we believe that the above estimates are very conservative upper limits.

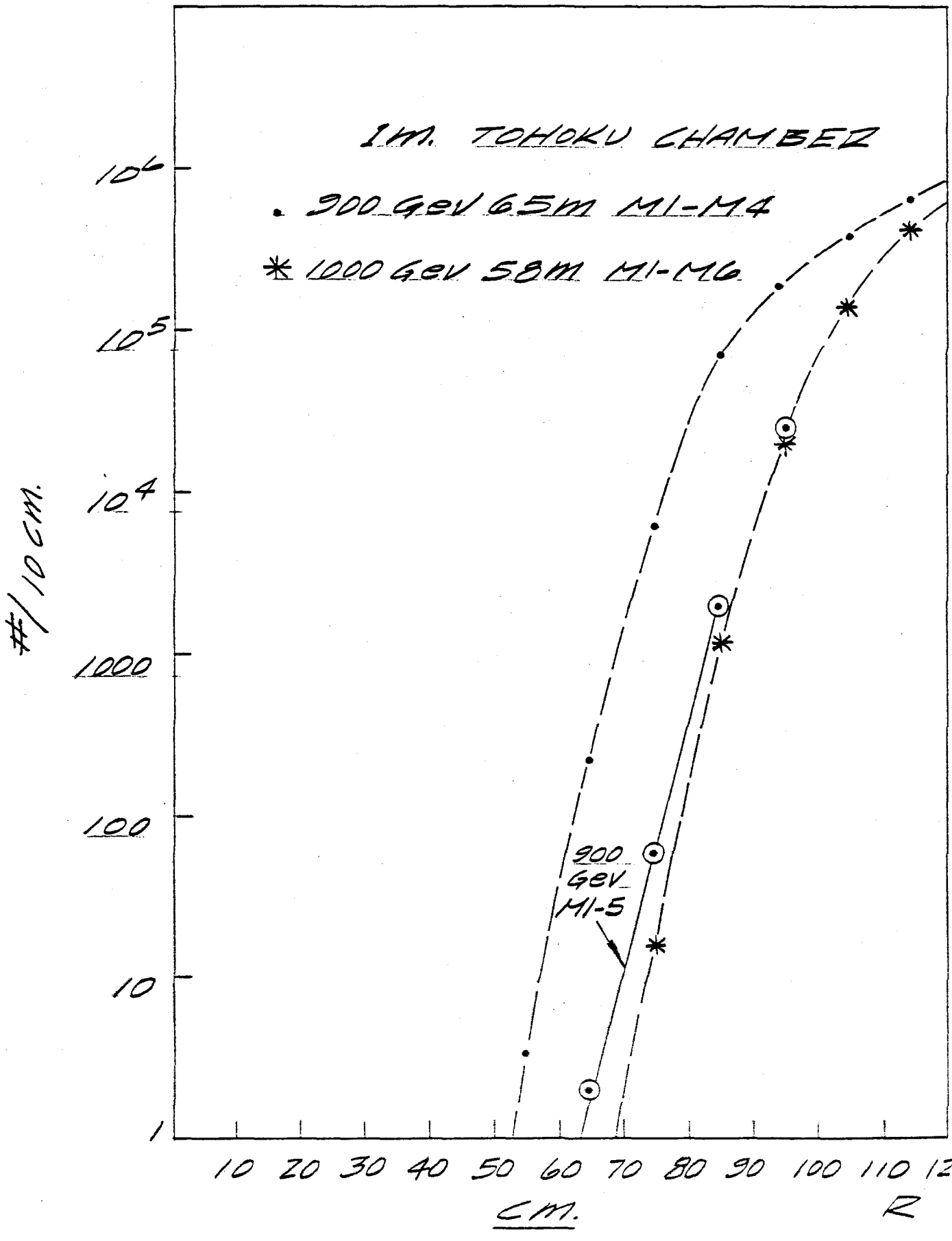
1M. TOHOKU CHAMBER
• 900 GeV 65M M1-M4
* 1000 GeV 58M M1-M6
900 GeV M1-5
#/10 CM.
CM.
R

Fig. V-1

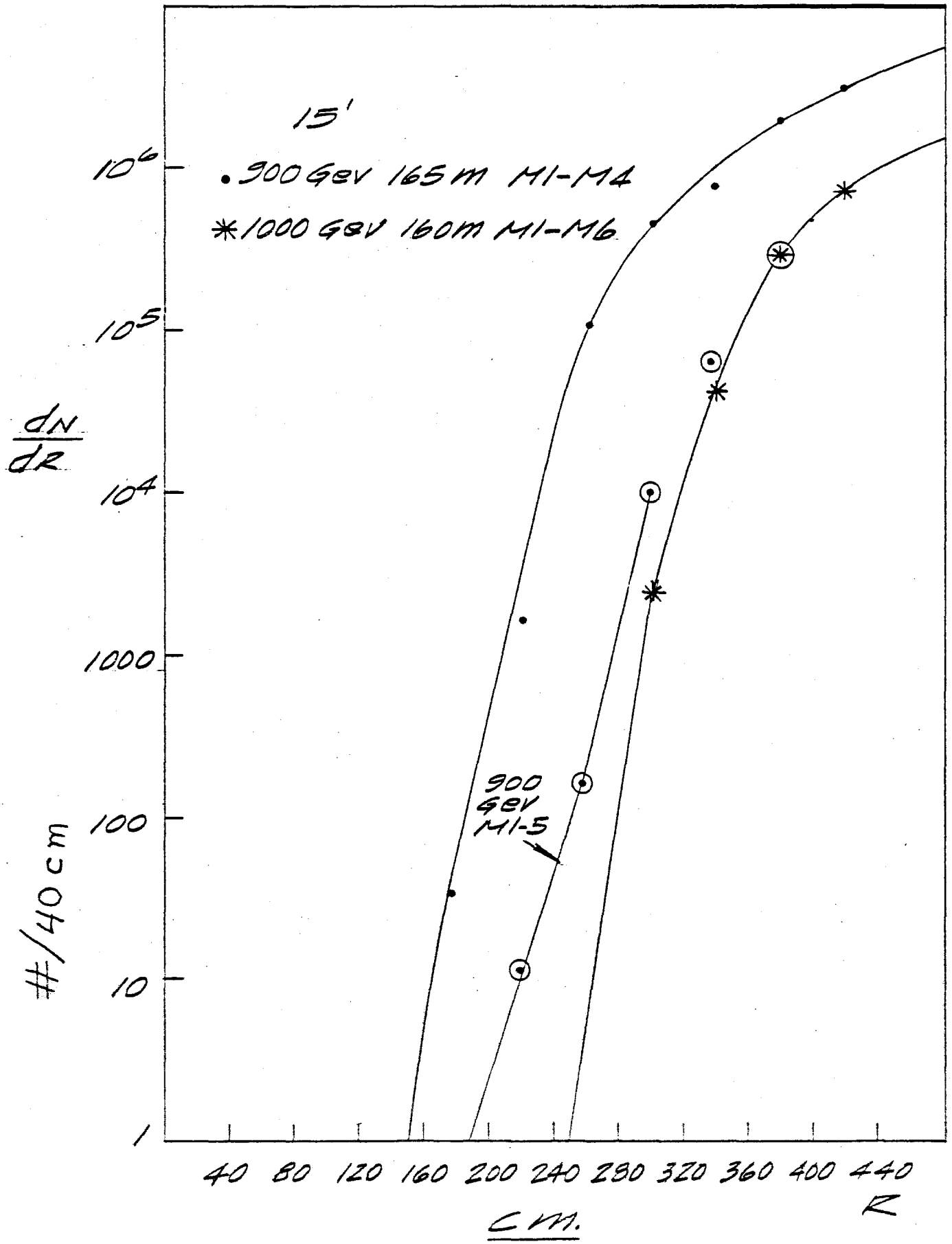
15'
• 900 GeV 165 m M1-M4
* 1000 GeV 160 m M1-M6
10^6
10^5
10^4
1000
100
10
1
$\frac{dN}{dR}$
#/40 cm
900 GeV M1-5
40 80 120 160 200 240 280 320 360 400 440
R
CM.

Fig. V-2

VI. Muon Fluxes Associated with the Proton Beam Transport

1. Beam Gas Interactions

We have examined the effects of proton beam interactions with the residual air of the vacuum system in the transport system. Pions and kaons produced in the air can decay to muons which traverse magnets and earth berm and reach the bubble chambers. The program HALO has been used to study this problem.

Proton-residual gas interactions were simulated by considering segments of 300' long to be lumped at the center of that particular segment. All dipoles and quadrupoles together with tunnel dimensions and external earth shielding were simulated in the calculation. The spatial and correlated angle and momentum distribution of muons arriving at a plane transverse to the beam at the location of the tungsten target is shown in Figure VI-1. This result is for interactions halfway between NE8 and NLA. Similar distributions for other source locations have been generated. These distributions of muons were then entered as input to the standard Monte Carlo program used for calculating muon fluxes from the tungsten dump. The output of that program gave muon fluxes in the detectors.

The results of the calculation are shown in Table VI-1. For pressures of 0.3μ upstream of NE8 and $\leq 0.03\mu$ throughout NE8 and down to the target the resulting muon fluxes are tolerable.

2. Beam Collimation

It can be seen from the previous discussion that fractional beam losses of $\leq 10^{-7}$ in NE8 are acceptable and somewhat less than this downstream of NE8. Beam losses 10^{-6} have been achieved in the proton transports for E-613 in the Meson Lab and prompt neutrino experiments at CERN. Due to the fact that the bubble chambers at CERN were protected by a full 400 GeV muon range shield, they experienced no difficulties. In the present case the situation is more difficult and great care must be exercised in minimizing beam losses.

To ensure low beam losses we must collimate the beam and eliminate halo at some point upstream of NE8. We have examined two possibilities; NW4 and the downstream end of NW1. We can interact halos of $\geq 10^{9}$ protons per pulse at both NW4 and the downstream end of NW1 with acceptably low muon fluxes in the detectors.

More work remains to be done on the final choice of locations of collimators and the optimum approach to achieving the required vacuum in the transport system. However, there are no insurmountable problems in the design of an adequately clean proton transport for the Direct Neutral Lepton Facility.

Table VI-1

	VACUUM	μ BACKGROUND	
		Muons/Pulse	
	Microns Pressure	1-m	15 Foot
NW1-NW4	0.3	0.4	1.3
NW4-NE8	0.3	0.4	1.2
NE8-NLA	0.03	0.2	1.8
NLA-NLB	0.03	0.3	0.3
	TOTAL	1.3	4.6

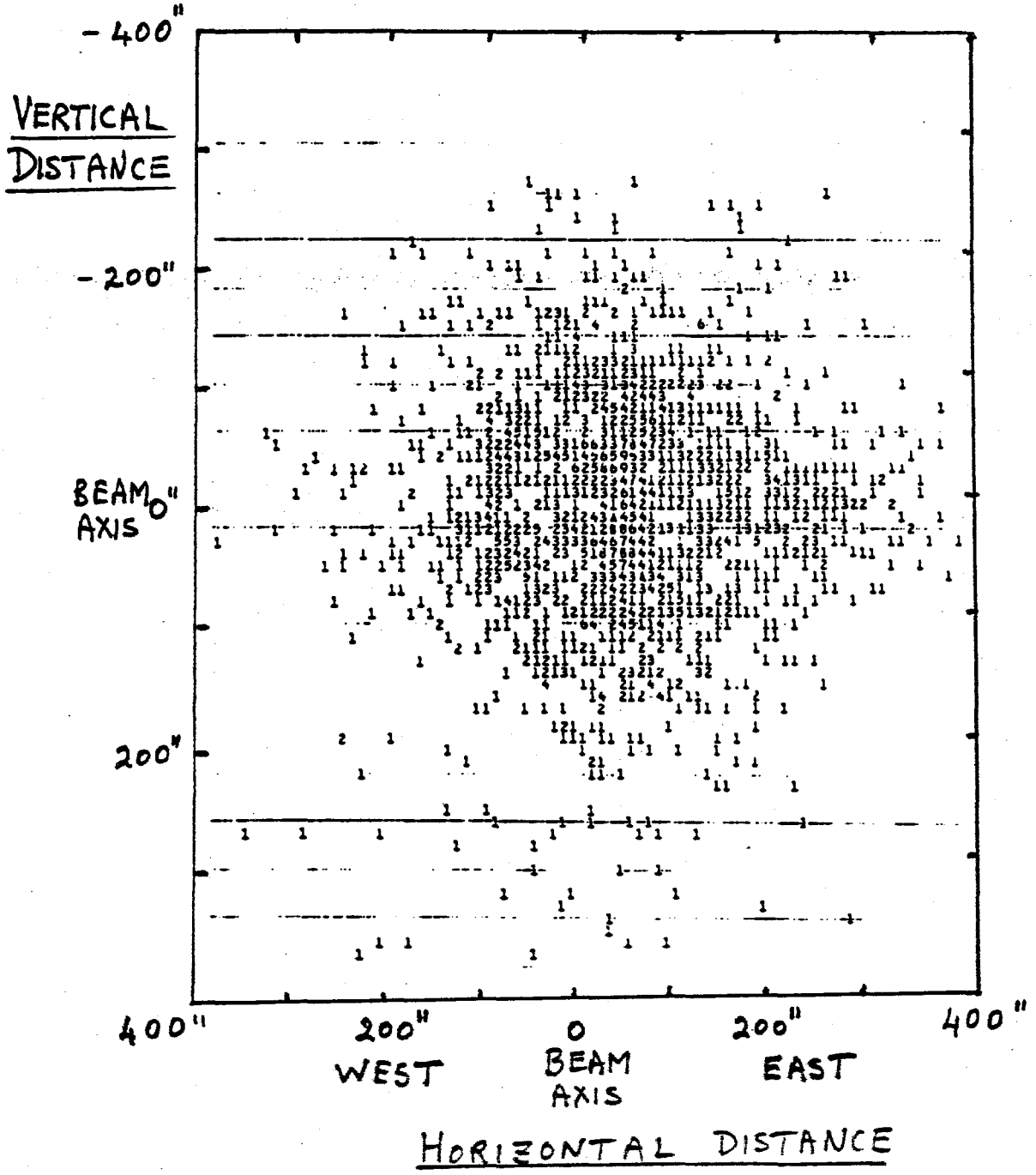

Negative muon spatial distribution in a plane transverse to the beam direction at the location of the tungsten target in NLB. The muons are produced by the interaction of 5×10^6 protons halfway between NE8 and NLA.

Fig. VI-1

Appendix

This appendix gives details of the equations used in the three beam dump Monte Carlo programs. For each class of formula the equations in each program will be detailed.

1 Energy Loss

1.1 Columbia

In Fe the Columbia program uses an energy dependent rate of energy loss given by:

$$\frac{dp}{dx} = \begin{cases} 1.327 + 2.418\times10^{-2}\,p - 3.8342\times10^{-4}\,p^2 & p < 30\ \text{GeV/c} \\ 1.592 + 5.169\times10^{-3}\,p + 6.971\times10^{-7}\,p^2 & p > 30\ \text{GeV/c} \end{cases}$$

$$\text{IN GeV/c /m}$$

In concrete a constant value is used:

$$\frac{dp}{dx} = .5 \ \text{GeV/c /m}$$

1.2 Fermilab

A calculated rate of restricted dE/dx for $dE/E < .1$ is used in the Fermilab progam. The values are shown in Figure A-1. Larger stochastic losses are randomly produced.

1.3 MIT

$$\left.\frac{dp}{dx}\right|_{Fe} = 1.16 + .13 \log p + 7.1\times10^{-6}(\log p)^7 \quad \text{GeV/c /m}$$

$$\left.\frac{dp}{dx}\right|_{conc} = \frac{.45}{1.16} \left.\frac{dp}{dx}\right|_{Fe}.$$

2 Pion Production

2.1 Columbia

$$E\frac{d^3\sigma}{dp^3} = A\frac{1}{(1+P_\perp^2/M^2)^4}(1-x_R)^n$$

$$x_R = E^*/E^*_{max}$$

	A	M^2	n
π^+	30.2	.66	3.2
π^-	17.4	.74	3.9

2.2 Fermilab

$$E\frac{d^3\sigma}{dp^3}\Big|^{A=1}_{\pi+} = 70\, e^{-7x_R}\frac{1}{(1+P_\perp^2/m^2)^{q^2}}$$

$$m^2 = .1 + 3.2x_R - 1.3x_R^2 \qquad q^2 = 3.5 + (8x_R - 4x_R^2 - .5)\left(\frac{.35}{1+e^{(P_\perp - 9.6)/1.8}} + .65\right)$$

$$\pi^-/\pi^+ = 1/(1.7 + 2.2x_\perp^2 + 9.1x_F^2)$$

$$\frac{d^3\sigma}{dp^3}\Big|^A \Big/ \frac{d^3\sigma}{dp^3}\Big|^1 = A^{.8-.3x_F+.15P_\perp}$$

2.3 MIT

The MIT progam does not separate muon production into pion production and subsequent decay or proportional direct muon production. The following equation is thus for muon production:

$$\frac{dN}{dE\,dp_x\,dp_y} = \alpha\frac{(1-E/E_o - P_\perp^2/2E)^4(1-E/E_o)}{E/E_o(1+P_\perp^2/.74)^{3.5}}$$

μ^-	$\frac{\alpha}{10^6/10^{12}\,p}$	AT 400 GeV E_o
μ^+	$1.5\times10^6/10^{12}\,p$	

3 Muon-pion Ratio

3.1 Columbia

$$\left.\frac{\mu}{\pi}\right|_{DIR} = 10^{-4}\,(1-x_F)^3$$

SHOWER MONTE CARLO

3.2 Fermilab

$$\left.\frac{\mu}{\pi^+}\right|_{DIR} = 10^{-4}\,(-1.91+.88\,\log E_{CM})\,(A/56)^{0.2}\,(1-x_F)^2 \qquad E_{CM} > 15.4\ \text{GeV}$$

$$R^{SHOWER}_{DIR} = 1+\left(.115/(E/E_{BEAM})\right)^{1.5} \qquad R^{SHOWER}_{DECAY} = 1+\left(.175/(E/E_{BEAM})\right)^{1.81}$$

3.3 MIT

See remarks above under pion production.

The production of muons from an Fe target as measured by Bodek et al and as calculated by the Columbia and Fermilab programs is shown in Figure A-2a. Figure A-2b compares the same data scaled to W with the values from the MIT program.

4 Coulomb Scattering

4.1 Columbia

The Columbia program uses standard Gaussian multiple scattering with:

$$\theta_{1/e} = \frac{.021}{p\beta}\sqrt{L/L_R}$$

4.2 Fermilab

The Fermilab progam uses a modification of the Moliere scattering formalism that takes into account the form factor of the iron nucleus. Figure A-3 gives the shapes of the scattering angle distributions used.

4.3 MIT

Standard multiple scattering:

$$\theta_{1/e} = \frac{.02}{E}\sqrt{L/L_R}$$

5 Inelastic Muon Scattering

5.1 Columbia

Similar to Fermilab

5.2 Fermilab

$$\frac{d^2\sigma}{dq^2\,d\nu} = \frac{2\pi\alpha^2}{p^2q^4}\,\frac{F_2(q^2,\nu)}{\nu}\left[2EE' - \frac{q^2}{2} + \frac{(q^2-2M_\mu^2)(1+\nu^2/q^2)}{1+R}\right]$$

$$F_2(q^2,\nu) = A(2+\epsilon_0)x(1-x)^{1+\epsilon_0} + B\,\frac{14(4+\epsilon_1)}{9(5+\epsilon_1)}(1-x)^{3+\epsilon_1}\,\frac{q^2}{q^2+m_0^2}$$

$$\epsilon_0 = G_{00} + \epsilon \qquad \epsilon_1 = G_{10} + \epsilon$$

$$\epsilon = K \log\left[(q^2+m_0^2)/m_0^2\right]$$

$A = .661 \quad B = .357 \quad K = .33 \quad G_{00} = 1.69 \quad G_{10} = 7.2 \quad m_0^2 = .573$

$R = .44$

5.3 MIT

$$\frac{d^2\sigma}{dE_2'\,d\Omega} = \frac{4\alpha^2E_2'}{q^4}\,W_2(q^2,x)\left[\frac{\sin^2\theta/2}{G(\nu,q^2)\,M} + \frac{x\cos^2\theta/2}{\nu}\right]$$

Figure A-4 compares calculations by the three programs with data from the EMC on the scattering of 280 GeV/c muons from 2.3 m of Fe.

6 Muon Trident Formation

All of the programs treat muon trident formation as a special kind of deep inelastic scattering, including a possible sign change of the produced muon.

6.1 Columbia

Uses the real photon process for muon pair production multiplied by a factor (a là Jack Smith) to take the virtual photon process (which is larger) into account.

6.2 Fermilab

$$\sigma(E) = \frac{\alpha}{2\pi}\left(\frac{Z}{6}\right)^2\left[\log\frac{E}{6.7m_\mu}\left(\log\frac{E}{6.7m_\mu}-\frac{3}{2}\right)\ln 3 \quad 1.52\,\mu b\right]$$

$$\frac{dN}{d\nu\, dM_{\mu\mu}} \propto \frac{1}{\nu}\, e^{-2M_{\mu\mu}}$$

6.3 MIT

$$\frac{d\sigma}{d\nu\, dQ^2} = \frac{\alpha}{\pi}\frac{1}{Q^2}\frac{1}{\sqrt{Q^2+\nu^2}}\left(\frac{Z}{6}\right)^2 1.52\,\mu b\,\frac{m_\mu^2}{m_\mu^2+Q^2}$$

$$\left[(1-\nu/E)(1-Q^2_{min}/Q^2)+\frac{\nu^2}{2E^2}+\frac{Q^2}{4E^2}\right]\log\frac{\nu}{6.2m_\mu^2}$$

FLAT ν DIST

COLLINEAR PRODUCTION

Appendix

Muon Production Formulae

1. The Muon Flux Formulae

a. The Columbia program started with the $\pi^{\pm}$ production formula obtained from a fit to the low $P_\perp$ data by Taylor and Walker:

$$E\frac{d\sigma}{d^3p} = C\frac{(1-x_R)^n}{(1+P_\perp^2/m^2)^4} \quad \text{mbarns/GeV/c}^2\text{/nucleon}$$

where $x_R \cong (1-x-P_\perp^2/2P_{||})$

and

	C	m^2	n
π^+	30.2	0.66	3.2
π^-	17.4	0.74	3.9

To obtain numbers of particles produced per interacting proton we correct for the fact that the total cross section goes like $A^{0.7}$ while high $P_\perp$ and large x π and μ production goes more like $A^{1.0}$

$$dn/dxd^2P_\perp = C \times \frac{A^{0.3}}{40\ \text{mb}} \frac{1}{x}\left(E\frac{d\sigma}{d^3p}\right)$$

These formulae were then multiplied by the μ/π ratios to obtain the μ fluxes. This ratio came from two processes:

i) Prompt muon production in the first collision of the proton (we call these direct 1 μ's). A fit to the experimental data (see Fig. A1) gives

$$\mu/\pi\big|_{\text{prompt}} = (1.0 \times 10^{-4})(1-x)^3 \quad .$$

ii) In a thick target we get additional muons from π and K decays in the hadronic cascade as well as additional prompt muons produced in the interactions of the pions in the hadronic cascade. These fluxes were calculated by a Monte Carlo program in which the hadronic cascade was followed and the muon flux from both prompt and decay sources were calculated. The resulting muon fluxes were then fitted to give (see Fig A1b)

$$\left.\frac{\mu}{\pi}\right|_{\substack{\text{Decays \& prompt}\\ \mu\text{'s in hadronic}\\ \text{cascade}}} = \left(\frac{350}{E_{prot}}\right)\left[(1.0\times10^{-4})(1-x)^3+(8.0\times10^{-4})e^{-23x}\right].$$

Combining these we get

$$\frac{dn\mu^+}{dx\,d^2p_\perp} = \frac{30.2\,A^{0.3}}{40}\,\frac{1}{x}\,\frac{(1-x_R)^{3.2}}{(1+P_\perp^2/0.66)^4}\,x\left\{\left[1.0\times10^{-4}(1-x)^3\right]\right.$$

$$\left. + \left(\frac{350}{E_{prot}}\right)\left[1.0\times10^{-4}(1-x)^3+8.0\times10^{-4}e^{-23x}\right]\right\}$$

and similarly for π^-. We see that once we get to $x \geq 0.1$ or so where the e^{-23x} is unimportant we have dependences like

$$\sim \frac{(1-x)^{6.2}}{(1+P_\perp^2/m^2)^4} \quad \text{for } \mu^+$$

$$\sim \frac{(1-x)^{6.9}}{(1+P_\perp^2/m^2)^4} \quad \text{for } \mu^- \ .$$

b. The Fermilab program used the $\pi^\pm$ production formula

$$E\frac{d\sigma(\pi^+)}{d^3p} = 70\ \frac{e^{-7x_R}}{(1+P_\perp{}^2/m^2)^n}$$

where

$$m^2 = 0.1 + 3.2\ x_R - 1.3\ x_R{}^2$$

$$n = 3.5 + (8x_R - 4x_R{}^2 - 0.5)\left(\frac{0.35}{1+e^{(P_\perp - 9.6)/1.8}} + 0.65\right)$$

$$\pi^-/\pi^+ = 1/(1.7+2.2\ x_\perp{}^2+9.1\ x_F{}^2)$$

$$\left.\frac{d\sigma}{d^3p}\right|_A = (A^{0.8-0.3x_F+0.15P_\perp})\left.\frac{d\sigma}{d^3p}\right|_{A=1}$$

The μ/π ratio was fitted to existing data (for the prompt part) and π and K decay contributions were calculated by a Monte Carlo program and then fitted, to yield

$$\left.\frac{\mu}{\pi}\right|_{\text{prompt}} = 10^{-4}(-1.91+0.88\ \log E_{cm})\left(\frac{A}{56}\right)^{0.2}(1-x_F)^2$$

The contributions from the hadronic cascade were expressed as

$$\left.\frac{\mu}{\pi}\right|_{\text{hadronic shower}} = (R_{\text{decay}}+R_{\text{direct}})\left.\frac{\mu}{\pi}\right|_{\text{prompt}}$$

$$R_{\text{direct}} = 1 + (0.115/(E/E_{\text{beam}}))^{1.5}$$

$$R_{\text{decay}} = 1 + (0.175/(E/E_{\text{beam}}))^{1.81}$$

c. The MIT program used a formula for muon production directly, based on a fit to the muon production data by W. Busza.

$$E\frac{dn\mu}{d^3p} = A(1-x)\frac{(1-x-P_\perp{}^2/2P_{||})^4}{(1+P_\perp{}^2/0.74)^{3.5}}$$

where $A = 6 \times 10^{-4}$ μ's/proton/GeV/c^2 for π^+ at 1000 GeV/c

$A = 4 \times 10^{-4}$ μ's/proton/GeV/c^2 for π^- at 1000 GeV/c

From calculating the E613 shield we found that this formula overestimated the μ flux at large x as well as at large $P_\perp$. The formula was therefore modified to

$$E\frac{dn\mu}{d^3p} = A\frac{(1-x_R)^6}{(1+P_\perp{}^2/0.74)^4} \quad \text{for } P_\perp < 3 \text{ GeV/c}$$

$$= A\frac{(1-x_R)^7}{(1+P_\perp{}^2/0.74)^4} \quad \text{for } P_\perp \geq 3 \text{ GeV/c} \ .$$

The MIT formula is intended to be valid for thick targets (dumps).

The predictions of the 3 formulae at 1000 Gev are compared in Fig. A7.

2. Comparison of the Muon Production Formulae with Measured Data.

a. The most relevant data for the total muon production is the data of Bodek, Ritchie et al. In this experiment, the total $\mu^\pm$ production rate was measured with 350 GeV protons in an iron beam dump. Jack Ritchie was very kind to supply us with this data before corrections were subtracted for π,K decays, etc. These numbers then can be directly compared to the total muon rates from our formulae, which is the quantity that is relevant to us. His numbers were for 6.038×10^8 protons interacting in the dump. He thought that the data were reliable for the region $P_\mu \geq 50$ GeV and $P_\perp \geq 0.6$ GeV/c. (continued on p. 10)

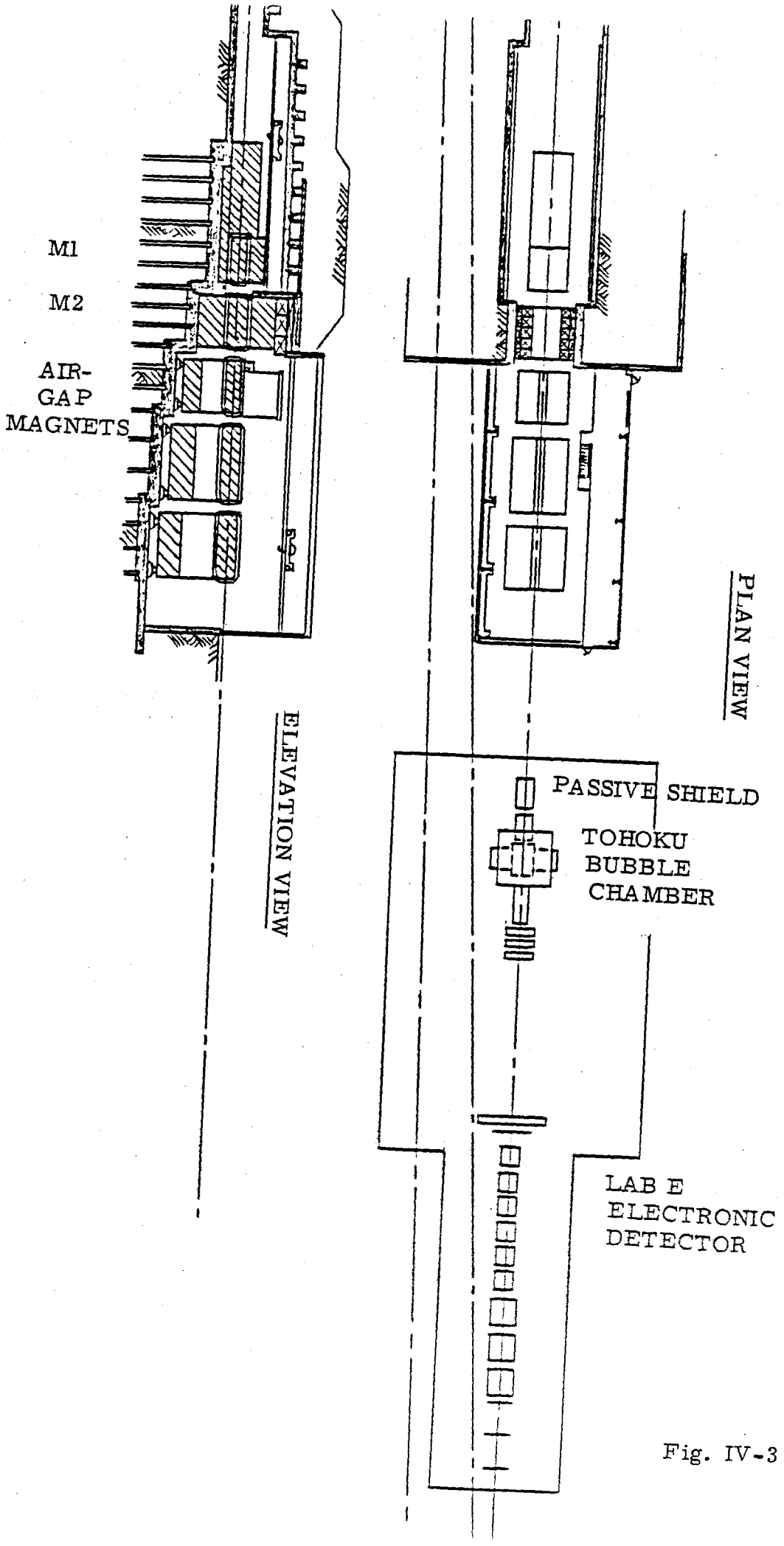
M1
M2
AIR-
GAP
MAGNETS
ELEVATION VIEW
PLAN VIEW
PASSIVE SHIELD
TOHOKU
BUBBLE
CHAMBER
LAB E
ELECTRONIC
DETECTOR

Fig. IV-3

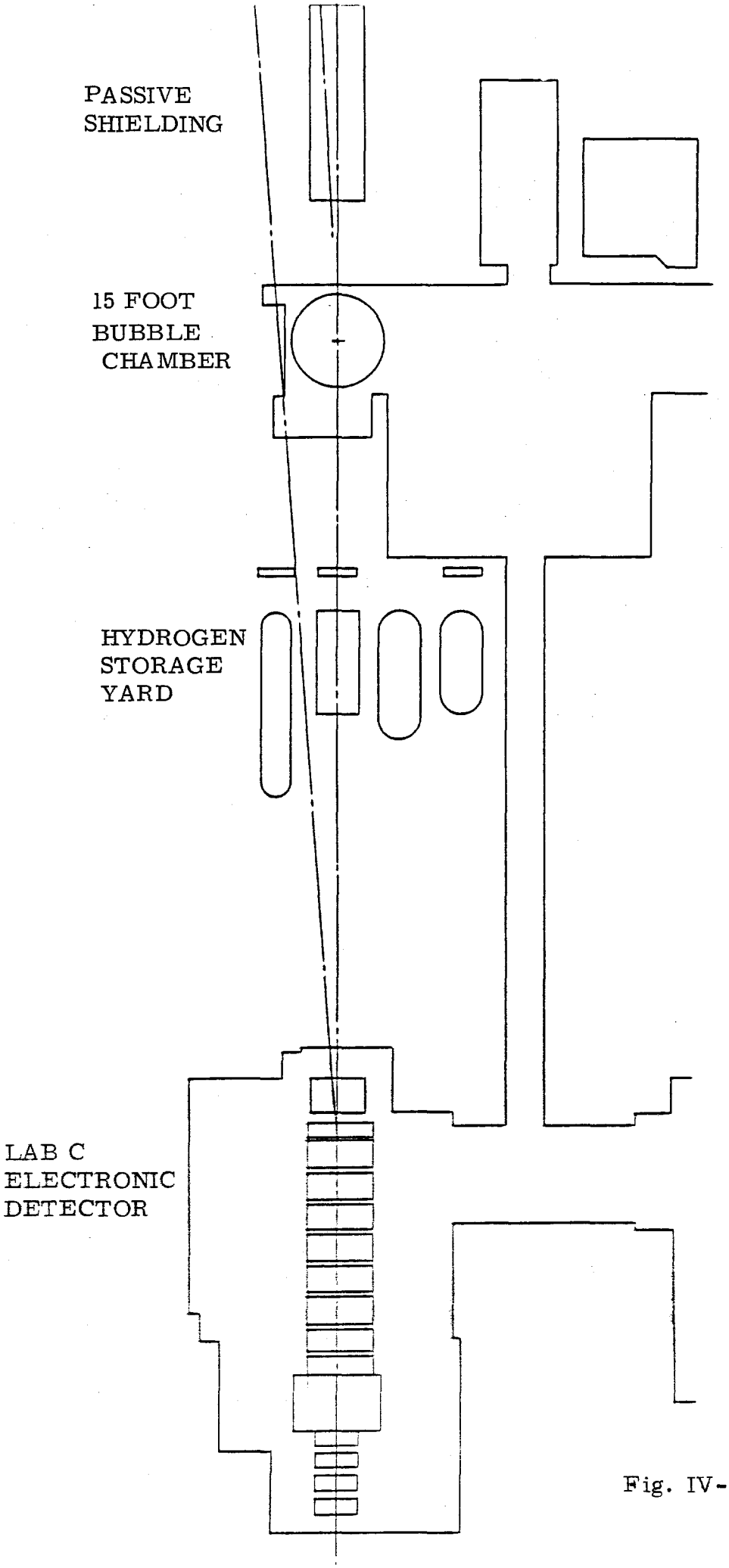
PASSIVE
SHIELDING
15 FOOT
BUBBLE
CHAMBER
HYDROGEN
STORAGE
YARD
LAB C
ELECTRONIC
DETECTOR

Fig. IV-4